RESEARCH ARTICLE | NOVEMBER 01 2024

An extended variational method for the resistive wall mode in toroidal plasma confinement devices

Special Collection: Celebrating the Contributions of Emeritus Professor Robert (Bob) Dewar

R. Fitzpatrick

Phys. Plasmas 31, 112502 (2024)
https://doi.org/10.1063/5.0239148

An extended variational method for the resistive wall mode in toroidal plasma confinement devices

Cite as: Phys. Plasmas **31**, 112502 (2024); doi: 10.1063/5.0239148
Submitted: 17 September 2024 · Accepted: 15 October 2024 ·
Published Online: 1 November 2024

R. Fitzpatrick[a)]

AFFILIATIONS

Institute for Fusion Studies, Department of Physics, University of Texas at Austin, Austin, Texas 78712, USA

Note: This paper is part of the Special Topic on Celebrating the Contributions of Emeritus Professor Robert (Bob) Dewar.
[a)]**Author to whom correspondence should be addressed:** rfitzp@utexas.edu

ABSTRACT

The external-kink stability of a toroidal plasma surrounded by a rigid resistive wall is investigated. The well-known analysis of Haney and Freidberg is rigorously extended to allow for a wall that is sufficiently thick that the thin-shell approximation does not necessarily hold. A generalized Haney–Freidberg formula for the growth-rate of the resistive wall mode is obtained. Thick-wall effects do not change the marginal stability point of the mode but introduce an interesting asymmetry between growing and decaying modes. Growing modes have growth-rates that exceed those predicted by the original Haney–Freidberg formula. On the other hand, decaying modes have decay-rates that are less than those predicted by the original formula. The well-known Hu–Betti formula for the rotational stabilization of the resistive wall mode is also generalized to take thick-wall effects into account. Increasing wall thickness facilitates the rotational stabilization of the mode, because it decreases the critical toroidal electromagnetic torque that the wall must exert on the plasma. On the other hand, the real frequency of the mode at the marginal stability point increases with increasing wall thickness.

I. INTRODUCTION

According to the standard ideal-magnetohydrodynamical (ideal-MHD) stability theory, a fusion plasma confined on a set of toroidally nested magnetic flux-surfaces can be rendered completely stable to ideal external-kink modes by means of a perfectly conducting, rigid wall that is located sufficiently close to the plasma boundary.[1–3] Of course, a practical metal wall possesses a finite electrical conductivity and can, therefore, only act as a perfect conductor on timescales that are much less than its characteristic L/R time. Given that the L/R time of any conceivable wall ($\approx 10^{-3}$ s) is considerably smaller than the desired confinement time of a fusion plasma (≈ 1 s),[4,5] it is clear that the finite conductivity of the wall must be taken into account in the stability analysis. When the finite wall conductivity is taken into consideration, ideal external-kink modes that would be stabilized by the wall, were it perfectly conducting, are found to grow on the L/R time of the wall.[6,7] Such comparatively slowly growing modes [compared to ideal external-kink modes, which grow on the extremely short ($\approx 10^{-7}$ s) Alfvén time][8–11] are known as *resistive wall modes*. In 1989, Haney and Freidberg[12] derived a very general formula for the growth-rate of a resistive wall mode that makes use of the "thin-shell approximation," according to which the skin-depth in the wall material is assumed to be much larger than the wall thickness. The aim of this paper is to generalize the Haney–Freidberg formula to allow for thicker walls in which the thin-shell approximation breaks down.[13–19]

The Haney–Freidberg formula features the quantity δW_{nw}, which represents the perturbed potential energy of the plasma calculated on the assumption that inertia is negligible and the wall is absent, as well as the quantity δW_{pw}, which represents the corresponding energy calculated on the assumption that the wall is present and perfectly conducting. The Haney–Freidberg calculation constructs the physical resistive wall mode eigenfunction as a linear superposition of the trial eigenfunctions that are used to calculate δW_{nw} and δW_{pw}. Now, the resistive wall mode eigenfunction must satisfy all physical boundary conditions at the plasma/vacuum interface. On the other hand, it turns out that the trial eigenfunctions do not satisfy the perturbed pressure balance boundary condition at the interface. In general, the only reason that δW_{nw} and δW_{pw} can take non-zero values is because this boundary condition is not satisfied. The fact that the trial eigenfunctions do not satisfy the pressure balance boundary condition is implicit in previous work, but has never been directly pointed out before. Furthermore, Haney and Freidberg did not explicitly demonstrate that their resistive wall mode eigenfunction satisfies the pressure balance

boundary condition (in general, it does). Consequently, the analysis presented in this paper will pay particular attention to the boundary conditions at the plasma/vacuum interface.

II. IDEAL EXTERNAL-KINK MODE STABILITY

A. Scenario

Section II reprises some well-known background material in order to closely examine relationship between δW_{nw} and δW_{pw} and the pressure balance boundary condition at the plasma/vacuum interface.

Consider a fusion plasma that is confined on a set of toroidally nested magnetic flux-surfaces. Let V_p represent the toroidal volume occupied by the plasma, and let S_p be the volume's bounding surface. Suppose that the plasma is surrounded by a rigid, conducting wall whose uniform thickness, d, is small compared to its effective minor radius, $\overline{b}$. Let the wall occupy the toroidal surface S_w. Let V_i represent the vacuum region lying between the plasma boundary and the wall. Finally, let V_o represent the vacuum region that lies outside the wall, and extends to infinity, see Fig. 1.

B. Plasma equilibrium

Let $\rho(\mathbf{r})$, $p(\mathbf{r})$, $\mathbf{B}(\mathbf{r})$, and $\mathbf{j}(\mathbf{r})$ represent the equilibrium plasma mass density, scalar pressure, magnetic field, and electric current density, respectively. It follows that $\mu_0\,\mathbf{j} = \nabla\times\mathbf{B}$, and $\nabla p = \mathbf{j}\times\mathbf{B}$. Let $\mathbf{n}$ be a unit, outward directed normal vector to S_p. We have

$$\mathbf{n}\cdot\mathbf{B} = 0 \tag{1}$$

on S_p, because S_p must correspond to a magnetic flux-surface. We also expect the rapid transport of particles and energy along magnetic field-lines to ensure that $\mathbf{n}\times\nabla p = 0$ on S_p.[5] Hence, we deduce from the equilibrium force balance equation that

$$\mathbf{n}\cdot\mathbf{j} = 0 \tag{2}$$

on S_p. Finally, equilibrium force balance across S_p yields

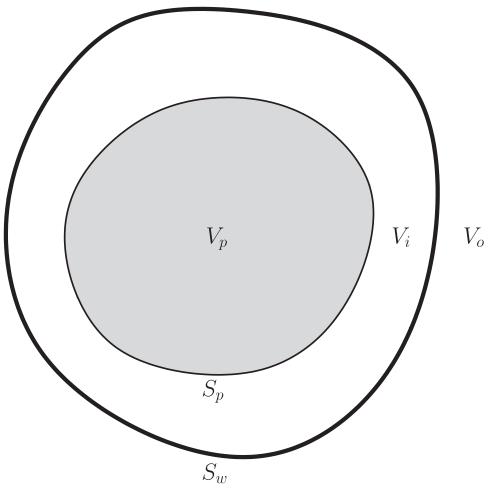

FIG. 1. Schematic diagram showing the poloidal cross section of a toroidally confined plasma. V_p is the plasma volume, and S_p is its bounding surface. S_w is a physically thin wall that surrounds the plasma. V_i is the vacuum region that lies between the plasma and the wall, whereas V_o is the vacuum region that lies outside the wall.

$$\left[\!\left[p + \frac{B^2}{2\,\mu_0}\right]\!\right] \equiv \frac{\hat{B}^2}{2\,\mu_0} - p - \frac{B^2}{2\,\mu_0} = 0 \tag{3}$$

on S_p, which implies that

$$\left[\!\left[\nabla\cdot\left(p + \frac{B^2}{2\,\mu_0}\right)\right]\!\right] = \left[\!\left[\mathbf{n}\cdot\nabla\left(p + \frac{B^2}{2\,\mu_0}\right)\right]\!\right]\mathbf{n} \tag{4}$$

on S_p. Here, $\hat{\mathbf{B}}(\mathbf{r})$ is the equilibrium magnetic field in the vacuum region.

C. Plasma perturbation

Assuming an $\exp(\gamma\,t)$ time dependence of all perturbed quantities, and neglecting equilibrium plasma flows, the perturbed, linearized plasma equation of motion takes the form[8–11]

$$\gamma^2\,\rho\,\boldsymbol{\xi} = \mathbf{F}(\boldsymbol{\xi}), \tag{5}$$

where

$$\mathbf{F}(\boldsymbol{\xi}) = \nabla(\Gamma\,p\,\nabla\cdot\boldsymbol{\xi}) - \mu_0^{-1}\,\mathbf{B}\times(\nabla\times\mathbf{Q}) + \nabla(\boldsymbol{\xi}\cdot\nabla p) + \mathbf{j}\times\mathbf{Q}, \tag{6}$$

and $\mathbf{Q} = \nabla\times(\boldsymbol{\xi}\times\mathbf{B})$. Here, $\boldsymbol{\xi}(\mathbf{r})$ is the plasma displacement, $\Gamma = 5/3$ is the ratio of specific heats, and $\mathbf{Q}(\mathbf{r})$ is the divergence-free perturbed magnetic field in the plasma. Moreover, $\mathbf{F}(\boldsymbol{\xi})$ is known as the *force operator*. The divergence-free perturbed magnetic field in the vacuum region is written as $\nabla\times\mathbf{A}$, where

$$\nabla\times(\nabla\times\mathbf{A}) = \mathbf{0}. \tag{7}$$

D. Physical boundary conditions

Now, $\boldsymbol{\xi}(\mathbf{r})$ must be square integrable at the magnetic axis, otherwise the potential energy, δW [see Eq. (12)], of the perturbation would be infinite. Furthermore,[9–11]

$$\mathbf{n}\times\mathbf{A} = -(\mathbf{n}\cdot\boldsymbol{\xi})\,\hat{\mathbf{B}}, \tag{8}$$

$$-\Gamma\,p\,\nabla\cdot\boldsymbol{\xi} + \boldsymbol{\xi}\cdot\nabla\left(\frac{B^2}{2\,\mu_0}\right) + \mu_0^{-1}\,\mathbf{B}\cdot\mathbf{Q} = \boldsymbol{\xi}\cdot\nabla\left(\frac{\hat{B}^2}{2\,\mu_0}\right) + \mu_0^{-1}\,\hat{\mathbf{B}}\cdot\nabla\times\mathbf{A} \tag{9}$$

on S_p. Equation (8) ensures that the perturbed plasma boundary remains a magnetic flux-surface, whereas Eq. (9) is an expression of perturbed pressure balance across the boundary. Finally, if the wall is perfectly conducting then

$$\mathbf{n}_w\times\mathbf{A} = \mathbf{0}, \tag{10}$$

on S_w, where $\mathbf{n}_w$ is a unit, outward directed normal vector to S_w. On the other hand, if the wall is absent then

$$\nabla\times\mathbf{A} = \mathbf{0}, \tag{11}$$

at infinity. Equation (10) ensures that the perturbed magnetic field cannot penetrate the perfectly conducting wall, whereas Eq. (11) ensures that the potential energy of the perturbation remains finite.

The boundary conditions (8), (10), and (11), the constraint that $\boldsymbol{\xi}(\mathbf{r})$ be square integrable at the magnetic axis, and the constraint that $\nabla \times \mathbf{A}$ be square integrable at infinity, are conventionally termed *essential boundary conditions*, whereas the boundary condition (10) is termed a *natural boundary condition*.[9–11] An essential boundary condition is one that must be satisfied by all prospective solution pairs $[\boldsymbol{\xi}(\mathbf{r}),\ \mathbf{A}(\mathbf{r})]$. In other words, an essential boundary condition must be satisfied by the physical resistive wall mode eigenfunction, as well as the trial eigenfunctions used to calculate δW_{nw} and δW_{pw}. On the other hand, a natural boundary condition is one that must be satisfied by the resistive wall mode eigenfunction, but can be violated by the trial eigenfunctions.

A more precise definition of a natural boundary condition is that it is one that emerges from the minimization of the plasma potential energy. In other words, the minimization processes drives the trial solution toward one that satisfies the boundary condition. Although this has been pointed out many times before,[8,10,11] what is not completely clear from previous work is that the minimization process can fail to satisfy a natural boundary condition if such satisfaction would overconstrain the problem. This is precisely what happens to the trial solutions used to calculate δW_{nw} and δW_{pw}.

E. Ideal-MHD energy principle

The potential energy of the perturbation characterized by the solution pair $[\boldsymbol{\xi}(\mathbf{r}),\ \mathbf{A}(\mathbf{r})]$ takes the form[8–11]

$$\delta W(\boldsymbol{\xi},\boldsymbol{\xi}) = -\frac{1}{2}\int_{V_p} \boldsymbol{\xi}\cdot\mathbf{F}(\boldsymbol{\xi})\,dV_p. \tag{12}$$

It follows from Eq. (A4) that

$$\delta W = \delta W_p + \delta W_s + \delta W_v, \tag{13}$$

where

$$\delta W_p(\boldsymbol{\xi},\boldsymbol{\xi}) = \frac{1}{2}\int_{V_p}\left[\Gamma p\,(\nabla\cdot\boldsymbol{\xi})\,(\nabla\cdot\boldsymbol{\xi}) + \mu_0^{-1}\,\mathbf{Q}\cdot\mathbf{Q} + (\nabla\cdot\boldsymbol{\xi})\,(\boldsymbol{\xi}\cdot\nabla p) + \mathbf{j}\cdot\boldsymbol{\xi}\times\mathbf{Q}\right]dV_p, \tag{14}$$

$$\delta W_s(\boldsymbol{\xi},\boldsymbol{\xi}) = \frac{1}{2}\int_{S_p}(\mathbf{n}\cdot\boldsymbol{\xi})\,(\mathbf{n}\cdot\boldsymbol{\xi})\,\mathbf{n}\cdot\left[\!\left[\nabla\left(p+\frac{B^2}{2\,\mu_0}\right)\right]\!\right]dS_p, \tag{15}$$

$$\delta W_v(\mathbf{A},\mathbf{A}) = \frac{1}{2\,\mu_0}\int_V (\nabla\times\mathbf{A})\cdot(\nabla\times\mathbf{A})\,dV. \tag{16}$$

Clearly, δW_p, δW_s, and δW_v, respectively, represent the contributions from the bulk plasma, from equilibrium surface currents flowing on the plasma boundary, and from the vacuum, to the overall potential energy of the perturbation.

The *ideal-MHD energy principle*[8–11] states that if any solution pair that satisfies the boundary conditions makes $\delta W < 0$ then the plasma is ideally unstable. In other words, at least one eigenmode with $\gamma^2 > 0$ exists, where γ is of order the inverse Alfvén time. On the other hand, if no valid solution pair can be found such that $\delta W < 0$ then the plasma is ideally stable. In other words, all eigenmodes are characterized by $\gamma^2 < 0$.

Clearly, in order to utilize the ideal-MHD principle, we need to minimize $\delta W(\boldsymbol{\xi},\boldsymbol{\xi})$ with respect to $\boldsymbol{\xi}$, and then determine whether the minimum value is positive or negative. In the former case, the plasma is ideally stable. In the latter case, it is ideally unstable. In Subsection 2 of the Appendix, it is shown that the trial solution pair that minimizes δW, subject to the essential boundary conditions, satisfies the force-balance equation,

$$\mathbf{F}(\boldsymbol{\xi}) = \mathbf{0}, \tag{17}$$

in V_p, satisfies Eq. (7) in V, and also ought to satisfy the pressure balance matching condition, (9), at the plasma boundary.

F. δW_{pw} and δW_{nw}

The perfect-wall and no-wall plasma potential energies, δW_{pw} and δW_{nw}, respectively, are defined in Subsection 3 of the Appendix. If $\delta W_{pw} > 0$ then the ideal external-kink mode in question is stabilized by the wall. On the other hand, if $\delta W_{nw} < 0$ then the ideal external-kink mode is unstable in the absence of the wall. Of course, the situation in which a kink mode is unstable in the absence of the wall, and stable in the presence of perfectly conducting wall, is exactly that which pertains to the resistive wall mode.

G. Relationship between δW_{nw}, δW_{pw} and pressure balance boundary condition

The reason that we have reproduced the very standard theory outlined in Secs. II B–II F is to make an important observation. Namely, the solution pairs $[\boldsymbol{\xi}(\mathbf{r}),\ \mathbf{A}_{pw}(\mathbf{r})]$ and $[\boldsymbol{\xi}(\mathbf{r}),\ \mathbf{A}_{nw}(\mathbf{r})]$, conventionally used to calculate δW_{pw} and δW_{nw}, respectively, do not satisfy the pressure balance matching condition, (9), at the plasma boundary. One way of seeing this is to note that if $\mathbf{F}(\boldsymbol{\xi}) = \mathbf{0}$ in V_p then, according to Eq. (12), $\delta W = 0$. However, if we assume that the pressure balance matching condition is not satisfied then Eq. (13) generalizes to

$$\delta W = \delta W_p + \delta W_s + \delta W_v + \delta W_c, \tag{18}$$

where

$$\delta W_c(\boldsymbol{\xi},\mathbf{A}) = \frac{1}{2}\int_{S_p}(\mathbf{n}\cdot\boldsymbol{\xi})\left[-\Gamma p\,\nabla\cdot\boldsymbol{\xi} + \boldsymbol{\xi}\cdot\nabla\left(\frac{B^2}{2\,\mu_0}\right) + \mu_0^{-1}\,\mathbf{B}\cdot\mathbf{Q} - \boldsymbol{\xi}\cdot\nabla\left(\frac{\hat{B}^2}{2\,\mu_0}\right) - \mu_0^{-1}\,\hat{\mathbf{B}}\cdot(\nabla\times\mathbf{A})\right]dS_p. \tag{19}$$

Here, the surface energy δW_c is directly related to the failure to satisfy the pressure balance matching condition at the plasma boundary. Thus, it is clear that

$$\delta W_{pw} = -\delta W_c(\boldsymbol{\xi},\mathbf{A}_{pw}), \tag{20}$$

$$\delta W_{nw} = -\delta W_c(\boldsymbol{\xi},\mathbf{A}_{nw}). \tag{21}$$

In other words, the only reason that δW_{pw} and δW_{nw} can take non-zero values at all is because the pressure balance matching condition is not satisfied, see Sec. IV L.

The fact that the solution pairs $[\boldsymbol{\xi}(\mathbf{r}),\ \mathbf{A}_{pw}(\mathbf{r})]$ and $[\boldsymbol{\xi}(\mathbf{r}),\ \mathbf{A}_{nw}(\mathbf{r})]$, do not satisfy the pressure balance matching condition, (9), at the plasma boundary is not problematic within the context of ideal-MHD theory. The ideal-MHD energy principle guarantees that if

$\delta W_{nw} < 0$ then we can find a solution of Eq. (5) inside the plasma, and Eq. (7) outside the plasma, which satisfies all of the boundary conditions in the absence of a wall, and is such that $\gamma^2 > 0$. Likewise, if $\delta W_{pw} > 0$ then we can find a solution of Eq. (5) inside the plasma, and Eq. (7) outside the plasma, which satisfies all of the boundary conditions in the presence of a perfectly conducting wall, and is such that $\gamma^2 < 0$. In both cases, the undetermined Alfvénic growth-rate of the instability, γ, provides the additional degree of freedom that allows the pressure balance matching condition, (9), to be satisfied at the plasma boundary. However, the analysis of Haney–Freidberg constructs the resistive wall mode solution from a linear combination of $[\boldsymbol{\xi}(\mathbf{r}), \mathbf{A}_{pw}(\mathbf{r})]$ and $[\boldsymbol{\xi}(\mathbf{r}), \mathbf{A}_{nw}(\mathbf{r})]$. Moreover, such a solution must satisfy all of the boundary conditions, including Eq. (9). Haney and Freidberg did not explicitly demonstrate that this is possible. As we shall see, it turns out that it is possible.

III. RESISTIVE WALL MODE PHYSICS

A. Resistive wall physics

Let $\mathbf{A}_i(\mathbf{r})$ be the vector potential in V_i. Let $\mathbf{A}_o(\mathbf{r})$ be the vector potential in V_o. Finally, let $\mathbf{A}_w(\mathbf{r})$ be the vector potential inside the wall. Choosing the Coulomb gauge within the wall,[20] the electric field in the wall takes the form $\mathbf{E}_w = -\gamma\,\mathbf{A}_w$, whereas the magnetic field is given by $\mathbf{B}_w = \nabla\times\mathbf{A}_w$. Ohm's law inside the wall yields $\mathbf{j}_w = \sigma_w\,\mathbf{E}_w$, where σ_w is the uniform electrical conductivity of the wall material, and $\mathbf{j}_w$ is the density of the electrical current flowing in the wall. Finally, $\mu_0\,\mathbf{j}_w = \nabla\times\mathbf{B}_w$. The previous equations can be combined to give

$$\nabla\times(\nabla\times\mathbf{A}_w) = -\mu_0\,\sigma_w\,\gamma\,\mathbf{A}_w. \tag{22}$$

Let d and $\overline{b}$ be the uniform thickness and effective minor radius of the wall, respectively. Now, we are assuming that the wall is physically thin: i.e., $d \ll \overline{b}$. Following Haney and Freidberg,[12] the position vector of a point lying within the wall is written $\mathbf{r} = \mathbf{r}_i + u\,d\,\mathbf{n}_w$. where $\mathbf{r}_i$ is the position vector of a point on the inner surface of the wall. The normalized length u represents perpendicular distance measured outward from the inner surface of the wall. Thus, $u=0$ and $u=1$ correspond to the inner and outer surface of the wall, respectively. We deduce that the gradient operator within the wall can be written as

$$\nabla = \frac{\mathbf{n}_w}{d}\frac{\partial}{\partial u} + \nabla_{S_w}, \tag{23}$$

where $\nabla_{S_w} \sim \overline{b}^{-1}$ only involves derivatives tangent to the surface of the wall.

To lowest order in $d/\overline{b}$, Eqs. (22) and (23) yield

$$\mathbf{n}_w\times\left(\mathbf{n}_w\times\frac{\partial^2\,\mathbf{A}_w}{\partial u^2}\right) = \lambda^2\,\mathbf{A}_w, \tag{24}$$

where $\lambda = \sqrt{\mu_0\,\sigma_w\,d^2\,\gamma}$. Let

$$\delta_\lambda = \frac{d}{\lambda\,\overline{b}}. \tag{25}$$

The neglect of tangential derivatives with respect to perpendicular derivatives in Eq. (24) is valid as long as $|\delta_\lambda| \ll 1$, which we shall assume to be the case. Note that $|\lambda| = d/d_{skin}$, where

$$d_{skin} = \frac{1}{\sqrt{\mu_0\,\sigma_w\,|\gamma|}} \tag{26}$$

is the skin-depth in the wall material.[20] The so-called *thin-shell* limit correspond to the situation in which the skin-depth is much greater than the wall thickness: i.e., $|\lambda| \ll 1$. On the other hand, the *thick-shell* limit corresponds to the situation in which the skin-depth is much greater than the wall thickness: i.e., $|\lambda| \gg 1$. Note that it is possible for the wall to be physically thin (i.e., $d/\overline{b} \ll 1$) but still be in the thick-shell limit.

Equation (24) yields

$$\frac{\partial^2}{\partial u^2}\,\mathbf{n}_w\times\mathbf{A}_w = \lambda^2\,\mathbf{n}_w\times\mathbf{A}_w. \tag{27}$$

The solution is

$$\mathbf{n}_w\times\mathbf{A}_w(u) = [\cosh(\lambda\,u) + \alpha\sinh(\lambda\,u)]\,\mathbf{n}_w\times\mathbf{A}_w(0), \tag{28}$$

where α is an arbitrary constant. Here, we have made the simplifying assumption that $\mathbf{A}_w(u)$ does not change direction across the wall: i.e., as u varies from 0 to 1. This assumption is certainly valid in the thin-shell limit, and we shall assume that it is also valid in the thick-shell limit. To the lowest order in δ_λ,

$$\begin{aligned}\nabla\times\mathbf{A}_w(u) &\simeq \frac{1}{d}\,\mathbf{n}_w\times\frac{\partial\mathbf{A}_w}{\partial u}\\ &= \frac{\lambda}{d}[\sinh(\lambda\,u) + \alpha\cosh(\lambda\,u)]\mathbf{n}\times\mathbf{A}_w(0).\end{aligned} \tag{29}$$

The boundary conditions that must be satisfied at the inner and outer surfaces of the wall are continuity of the tangential component of the electric field,[20] and continuity of the tangential component of the magnetic field. The latter boundary condition follows because we are assuming that there are no sheet currents flowing on the inner or the outer surface of the wall.[12] Thus, we obtain

$$\mathbf{n}_w\times\mathbf{A}_i = \mathbf{n}_w\times\mathbf{A}_w(0), \tag{30}$$

$$\mathbf{n}_w\times\mathbf{A}_o = \mathbf{n}_w\times\mathbf{A}_w(1) = (\cosh\lambda + \alpha\sinh\lambda)\,\mathbf{n}\times\mathbf{A}_i, \tag{31}$$

$$\overline{b}\,\mathbf{n}_w\times(\nabla\times\mathbf{A}_i) = \overline{b}\,[\mathbf{n}_w\times(\nabla\times\mathbf{A}_w)](0) \simeq \delta_\lambda^{-1}\,\alpha\,\mathbf{n}_w\times(\mathbf{n}_w\times\mathbf{A}_i), \tag{32}$$

$$\begin{aligned}\overline{b}\,\mathbf{n}_w\times(\nabla\times\mathbf{A}_o) &= \overline{b}\,[\mathbf{n}_w\times(\nabla\times\mathbf{A}_w)](1)\\ &\simeq \delta_\lambda^{-1}\,(\sinh\lambda + \alpha\cosh\lambda)\,\mathbf{n}_w\times(\mathbf{n}_w\times\mathbf{A}_i)\\ &= \delta_\lambda^{-1}\left(\frac{\sinh\lambda+\alpha\cosh\lambda}{\cosh\lambda+\alpha\sinh\lambda}\right)\mathbf{n}_w\times(\mathbf{n}_w\times\mathbf{A}_o),\end{aligned} \tag{33}$$

where use has been made of Eqs. (25), (28), and (29). Here, $\mathbf{A}_i$ and $\mathbf{A}_o$ are evaluated on the inner and outer surfaces of the wall, respectively.

Let

$$\zeta_o = \frac{\overline{b}\,\mathbf{n}_w\times(\nabla\times\mathbf{A}_o)}{\mathbf{n}_w\times(\mathbf{n}_w\times\mathbf{A}_o)}. \tag{34}$$

Note that ζ_o must be a scalar in order to satisfy Eq. (33). Now, we expect $\mathbf{A}_o$ to decay monotonically to zero as we move from the outer surface of the wall to infinity. Moreover, we expect the decay length to be of order $1/\overline{b}$. It follows that $\zeta_o \sim \mathcal{O}(1)$.

Equations (33) and (34) can be combined to give

$$\delta_\lambda \zeta_o = \frac{\sinh\lambda + \alpha\cosh\lambda}{\cosh\lambda + \alpha\sinh\lambda}, \tag{35}$$

which implies that[15]

$$\alpha = -\tanh\lambda + \frac{\delta_\lambda \zeta_o}{\cosh^2\lambda} + \mathcal{O}(\delta_\lambda \zeta_o)^2. \tag{36}$$

To lowest order in $\delta_\lambda \zeta_o$, Eqs. (31), (32), and (34) yield

$$\mathbf{n}_w \times \mathbf{A}_o = \frac{\mathbf{n}_w \times \mathbf{A}_i}{\cosh\lambda}, \tag{37}$$

$$\mathbf{n}_w \times (\nabla \times \mathbf{A}_i) = -\frac{\lambda\tanh\lambda}{d}\,\mathbf{n}_w \times (\mathbf{n}_w \times \mathbf{A}_i) + \frac{\mathbf{n}_w \times (\nabla \times \mathbf{A}_o)}{\cosh\lambda}. \tag{38}$$

The previous equation gives

$$\mathbf{n}_w \times [\mathbf{n}_w \times (\nabla \times \mathbf{A}_i)] = \frac{\lambda\tanh\lambda}{d}\,\mathbf{n}_w \times \mathbf{A}_i + \frac{\mathbf{n}_w \times [\mathbf{n}_w \times (\nabla \times \mathbf{A}_o)]}{\cosh\lambda}. \tag{39}$$

Equations (37) and (38) [or, alternatively, Eq. (39)] are the two matching conditions that must be satisfied at the wall. According to Eq. (37), $|\mathbf{n}_w \times \mathbf{A}_o| \simeq |\mathbf{n}_w \times \mathbf{A}_i|$ in the thin-shell limit.[12] On the other hand, $|\mathbf{n}_w \times \mathbf{A}_o| \ll |\mathbf{n}_w \times \mathbf{A}_i|$ in the thick-shell limit, due to the shielding of the outer vacuum region, V_o, from the inner vacuum region, V_i, by eddy currents excited in the wall. (See Fig. 2.) Finally, Eqs. (37) and (39) can be combined to produce

$$\mathbf{n}_w \times \mathbf{A}_i \cdot \mathbf{n}_w \times [\mathbf{n}_w \times (\nabla \times \mathbf{A}_i)] = \mathbf{n}_w \times \mathbf{A}_o \cdot \mathbf{n}_w \times [\mathbf{n}_w \times (\nabla \times \mathbf{A}_o)] + \frac{\lambda\tanh\lambda}{d}\,|\mathbf{n}_w \times \mathbf{A}_i|^2. \tag{40}$$

Figure 2 shows how $\mathbf{n}_w \times \mathbf{A}_w$ varies across a wall for various different choices of the ratio of the wall thickness to the skin-depth, λ. It can be seen that in the thin-shell limit, $\lambda \ll 1$, $\mathbf{n}_w \times \mathbf{A}$ only exhibits weak variation across the wall, whereas in the thick-shell limit, $\lambda \gg 1$, $\mathbf{n}_w \times \mathbf{A}$ decays to almost zero from the inner to the outer surface of the wall.

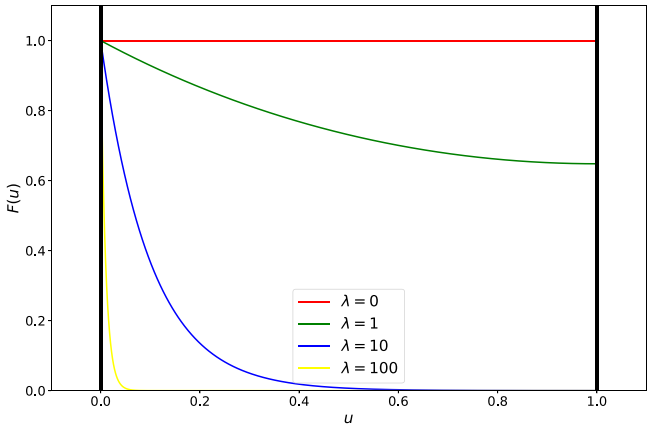

FIG. 2. Variation of $F(u) = [\mathbf{n}_w \times \mathbf{A}_w(u)]/[\mathbf{n}_w \times \mathbf{A}_w(0)]$ across a resistive wall for various values of the ratio, λ, of the wall thickness to the skin-depth in the wall material. Here, the scaled perpendicular distance, u, takes the value 0 on the inner surface of the wall, and 1 on the outer surface.

B. Timescale ordering

In order for the left-hand side of Eq. (5) to compete with the right-hand side, we need $\gamma \sim \tau_A^{-1}$, where $\tau_A \simeq \sqrt{\mu_0\,\rho\,a^2/B^2} \sim 10^{-7}$ s. Here, a is the minor radius of the plasma. However, the growth-rate of a resistive wall mode is of order $\overline{\tau}_w^{-1}$, where $\overline{\tau}_w \simeq \mu_0\,\sigma_w\,d\,\overline{b} \gtrsim 10^{-3}$ s.[6,7,12] Hence, it is clear that, for the case of a resistive wall mode, the left-hand side of Eq. (5) is negligible. In other words, plasma inertia is negligible. Consequently, the plasma displacement associated with the resistive wall mode satisfies the force balance equation, (17), within the plasma. Note that we are saying that the actual physical solution, as opposed to a trial solution, must satisfy Eq. (17) within the plasma.

C. Variational principle

In Subsection 4 of the Appendix, we confirm that the force operator is self-adjoint in the presence of a thick resistive wall. Making use of Eq. (A23), the perturbed potential energy of the resistive wall mode can be written as

$$\delta W(\boldsymbol{\xi},\boldsymbol{\xi}) = -\frac{1}{2}\int_{V_p} \boldsymbol{\xi}\cdot\mathbf{F}(\boldsymbol{\xi})\,dV_p = \delta W_p + \delta W_s + \delta W_v^{(i)} + \delta W_v^{(o)} + \delta W_v^{(w)}, \tag{41}$$

where

$$\delta W_v^{(i)}(\mathbf{A}_i,\mathbf{A}_i) = \frac{1}{2\,\mu_0}\int_{V_i} (\nabla\times\mathbf{A}_i)^2\,dV_i, \tag{42}$$

$$\delta W_v^{(o)}(\mathbf{A}_o,\mathbf{A}_o) = \frac{1}{2\,\mu_0}\int_{V_o} (\nabla\times\mathbf{A}_o)^2\,dV_o, \tag{43}$$

$$\delta W_v^{(w)}(\mathbf{A}_i,\mathbf{A}_i) = \frac{\lambda\tanh\lambda}{d}\,\frac{1}{2\,\mu_0}\int_{S_w} |\mathbf{A}_i\times\mathbf{n}_w|^2\,dS_w. \tag{44}$$

Clearly, $\delta W_v^{(i)}$ is the potential energy associated with the vacuum region interior to the wall, $\delta W_v^{(o)}$ is the potential energy associated with the vacuum region exterior to the wall, and $\delta W_v^{(w)}$ is the potential energy associated with eddy currents excited in the wall. In fact, it is easily demonstrated that

$$\delta W_v^{(w)} = \gamma^{-1}\int_{V_w} \mathbf{j}_w\cdot\mathbf{E}_w\,dV_w, \tag{45}$$

where V_w represents the volume occupied by the wall. In deriving the previous formula, we have assumed that $\mathbf{n}_w\cdot\mathbf{A}_w \simeq 0$ in V_w, which implies that the eddy currents excited in the wall flow predominately in directions tangental to the wall surface (because $d \ll \overline{b}$). Incidentally, can be shown that the magnetic energy of the wall, $(1/2\,\mu_0)\int_{V_w}|\nabla\times\mathbf{A}_w|^2\,dV_w$, is negligible.

Given that Eq. (17) holds within the plasma, it is clear that from Eq. (12) that

$$\delta W = 0 \tag{46}$$

for a resistive wall mode. This is not a surprising result, because a resistive wall mode is essentially a marginally stable ideal mode (given that $|\gamma| \ll \tau_A^{-1}$), which corresponds to a mode with $\delta W = 0$.

In Subsection 5 of the Appendix, it is shown that the solution pair $[\boldsymbol{\xi}(\mathbf{r}), \mathbf{A}(\mathbf{r})]$, that minimizes the $\delta W(\boldsymbol{\xi}, \boldsymbol{\xi})$ specified in Eq. (41), while satisfying the essential boundary conditions, satisfies Eq. (17) in V_p, satisfies Eq. (7) in V_i and V_o, satisfies the pressure balance matching condition, (9), at the plasma boundary, and satisfies the matching condition (39) at the wall. In other words, the solution pair solves the resistive wall mode problem.

Note that the wall matching condition (37) is clearly an essential boundary condition, whereas the matching condition (38) [or, alternatively, (39)] plays the role of a natural boundary condition.[10]

We might ask why we believe that the solution pair that minimizes the $\delta W(\boldsymbol{\xi}, \boldsymbol{\xi})$ specified in Eq. (41) will satisfy the pressure balance matching condition, (9), at the plasma boundary, when the solution pair that minimizes the $\delta W(\boldsymbol{\xi}, \boldsymbol{\xi})$ specified in Eq. (13) failed to do this. The answer is that the unspecified growth-rate of the resistive wall mode, γ, introduces an additional degree of freedom into the system that allows us to simultaneously satisfy all of the boundary conditions.

D. Minimization process

Following Haney and Freidberg,[12] let us write

$$\mathbf{A}_i(\mathbf{r}) = c_1\, \mathbf{A}_{nw}(\mathbf{r}) + c_2\, \mathbf{A}_{pw}(\mathbf{r}), \tag{47}$$

$$\mathbf{A}_o(\mathbf{r}) = c_3\, \mathbf{A}_{nw}(\mathbf{r}), \tag{48}$$

where c_1, c_2, and c_3 are constants that must be determined by the essential boundary conditions and the minimization process. Now, the essential boundary condition (8) implies that

$$\mathbf{n} \times \mathbf{A}_i = -(\mathbf{n} \cdot \boldsymbol{\xi})\, \hat{\mathbf{B}} \tag{49}$$

on S_p. Combining this relation with Eqs. (A13), (A17), and (47), we deduce that

$$c_1 + c_2 = 1. \tag{50}$$

Next, the essential boundary condition (37) can be combined with Eqs. (A14), (47), and (48) to give

$$c_3 = \frac{c_1}{\cosh\lambda}. \tag{51}$$

Note that the essential boundary condition (11) is automatically satisfied because of Eq. (A18).

The useful results listed in Subsection 6 of the Appendix can be combined to give the following expression for the vacuum energy:

$$\begin{aligned}\delta W_v &= \delta W_v^{(i)} + \delta W_v^{(o)} + \delta W_v^{(w)}\\ &= \delta W_v^{(\infty)} + c_2^2\,(\delta W_v^{(b)} - \delta W_v^{(\infty)})\\ &\quad + (1-c_2)^2 \left[\frac{\lambda\tanh\lambda}{2\,\mu_0\,d}\int_{S_w} |\mathbf{A}_{nw}\times\mathbf{n}_w|^2\, dS_w - \tanh^2\lambda\,\delta W_v^{(x)}\right].\end{aligned} \tag{52}$$

Here, $\delta W_v^{(x)}$ represents the contribution of the region V_o to the no-wall vacuum energy, and is defined in Eq. (A34). Now, the ratio of the first term to the second term appearing in square brackets in the previous equation is roughly $\overline{b}\,\lambda/(d\tanh\lambda)$. Thus, in the thin-shell limit, $\lambda \ll 1$, the ratio is $\overline{b}/d$, which is very large. On the other hand, in the thick-shell limit, $\lambda \gg 1$, the ratio is δ_λ^{-1} [see Eq. (25)], which is also very large. Hence, we deduce that we can neglect the second term. Thus, the previous equation simplifies to give

$$\delta W_v = \delta W_v^{(\infty)} + c_2^2\,(\delta W_v^{(b)} - \delta W_v^{(\infty)}) + (1-c_2)^2\, F(\lambda), \tag{53}$$

where

$$F(\lambda) = \frac{\lambda\tanh\lambda}{2\,\mu_0\,d}\int_{S_w} |\mathbf{A}_{nw}\times\mathbf{n}_w|^2\, dS_w. \tag{54}$$

According to the variational principle discussed in Sec. III C, we can determine the true vacuum energy by minimizing δW_v with respect to variations in c_2. This procedure yields

$$c_2 = \frac{F(\lambda)}{\delta W_v^{(b)} - \delta W_v^{(\infty)} + F(\lambda)}, \tag{55}$$

$$\delta W_v = \delta W_v^{(\infty)} + \frac{(\delta W_v^{(b)} - \delta W_v^{(\infty)})\, F(\lambda)}{\delta W_v^{(b)} - \delta W_v^{(\infty)} + F(\lambda)}. \tag{56}$$

Following Haney and Freidberg,[12] we can define the effective minor radius of the wall as

$$\overline{b} = \frac{(1/2\,\mu_0)\displaystyle\int_{S_w} |\mathbf{A}_{nw}\times\mathbf{n}_w|^2\, dS_w}{\delta W_v^{(b)} - \delta W_v^{(\infty)}}. \tag{57}$$

Equations (54) and (57) give

$$\delta W_v = \delta W_v^{(\infty)} + (\delta W_v^{(b)} - \delta W_v^{(\infty)})\,\frac{G(\gamma)}{1+G(\gamma)}, \tag{58}$$

where

$$G(\gamma) = \sqrt{\frac{\gamma\,\overline{\tau}_w}{\overline{\delta}_w}}\tanh\left(\sqrt{\overline{\delta}_w\,\gamma\,\overline{\tau}_w}\right), \tag{59}$$

$$\overline{\tau}_w = \mu_0\,\sigma_w\,d\,\overline{b}, \tag{60}$$

$$\overline{\delta}_w = \frac{d}{\overline{b}}. \tag{61}$$

Here, $\overline{\tau}_w$ is the effective L/R time of the wall, whereas $\overline{\delta}_w \ll 1$ measures the relative wall thickness.

E. Generalized Haney–Freidberg formula

According to Eqs. (41), (52), and (58), the total potential energy of the perturbation is

$$\delta W = \delta W_p + \delta W_s + \delta W_v = \delta W_{nw} + (\delta W_{pw} - \delta W_{nw})\,\frac{G(\gamma)}{1+G(\gamma)}, \tag{62}$$

where use has been made of Eqs. (A11) and (A15). However, Eq. (46) mandates that $\delta W = 0$ for a resistive wall mode, so we obtain the following *generalized Haney–Freidberg formula*:

$$\sqrt{\frac{\gamma\,\overline{\tau}_w}{\overline{\delta}_w}}\tanh\left(\sqrt{\overline{\delta}_w\,\gamma\,\overline{\tau}_w}\right) = -\frac{\delta W_{nw}}{\delta W_{pw}}, \tag{63}$$

for the case $\delta W_{nw} < 0$, $\delta W_{pw} > 0$ in which the resistive wall mode is unstable, and

$$\sqrt{\frac{-\gamma\,\overline{\tau}_w}{\overline{\delta}_w}}\,\tan\left(\sqrt{-\overline{\delta}_w\,\gamma\,\overline{\tau}_w}\right) = \frac{\delta W_{nw}}{\delta W_{pw}} \tag{64}$$

for the case $\delta W_{nw} > 0$, $\delta W_{pw} > 0$ in which the resistive wall mode is stable. The formula does not apply to the case $\delta W_{pw} < 0$ in which the plasma is ideally unstable in the presence of the wall, because the neglect of plasma inertia is not tenable in this situation. The derivation of the generalized Haney–Freidberg formula is valid provided

$$\frac{d}{\overline{b}} \ll |\gamma|\,\overline{\tau}_w,\ 1. \tag{65}$$

In the thin-shell limit, $\overline{\delta}_w\,|\gamma|\,\overline{\tau}_w \ll 1$, Eqs. (63) and (64) reduce to the original Haney–Freidberg formula:

$$\gamma\,\overline{\tau}_w = -\frac{\delta W_{nw}}{\delta W_{pw}}. \tag{66}$$

Equations (46), (50), (55), and (62) yield

$$c_1 = \frac{\delta W_{pw}}{\delta W_{pw} - \delta W_{nw}}, \tag{67}$$

$$c_2 = -\frac{\delta W_{nw}}{\delta W_{pw} - \delta W_{nw}}. \tag{68}$$

Moreover, given that the generalized Haney–Freidberg dispersion relation sets $\delta W = 0$, a comparison of Eqs. (18) and (62) reveals that $\delta W_c = 0$, where δW_c is defined in Eq. (19). Thus, the linear combination of solutions, (47), with c_1 and c_2 given by the previous two equations, ensures that the pressure balance matching condition, (9), is satisfied at the plasma boundary. Later on, in Sec. IV N, we shall show a particular example of this.

F. Resistive wall mode growth-rate

Figure 3 shows the growth-rate of the resistive wall mode predicted by the generalized Haney–Freidberg formula, (63) and (64). For a thin wall characterized by $\overline{\delta}_w \ll 1$, we reproduce the characteristic linear relationship between $\gamma\,\overline{\tau}_w$ and $-\delta W_{nw}/\delta W_{pw}$ predicted by the original Haney–Freidberg formula. The mode grows or decays on the characteristic L/R timescale, $\overline{\tau}_w$, and the marginal stability point, $\delta W_{nw} = 0$, is the same as that for an ideal-kink mode in the absence of a wall.[6] Thick-wall effects, which manifest themselves when $\overline{\delta}_w \lesssim 1$, do not change the marginal stability point, in accordance with a result first proved by Pfirsch and Tasso in 1971,[6] but introduce an interesting asymmetry between growing and decaying modes. Growing modes have growth-rates that exceed those predicted by the original Haney–Freidberg formula. (Here, we are comparing thick and thin walls with the same $\overline{\tau}_w$ values.) On the other hand, decaying modes have decay-rates that are less than those predicted by the original formula. Note that there are actually multiple branches of decaying solutions, and we have plotted the most slowly decaying branch in Fig. 3.

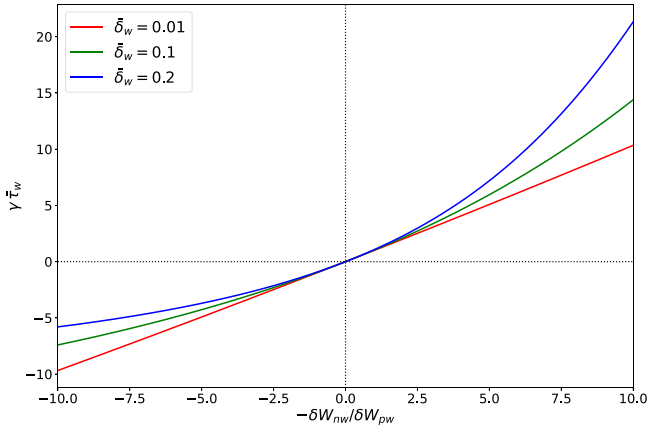

FIG. 3. Growth-rate of the resistive wall mode predicted by the generalized Haney–Freidberg formula, (63).

For a very rapidly growing resistive wall mode, such that $\gamma\,\overline{\tau}_w\,\overline{\delta}_w \gg 1$, which corresponds to the complete breakdown of the thin-shell approximation, Eq. (63) reduces to[13,17]

$$\gamma\,\overline{\tau}_w = \overline{\delta}_w\left(-\frac{\delta W_{nw}}{\delta W_{pw}}\right)^2. \tag{69}$$

In this limit, the mode is almost completely shielded from the vacuum region outside the wall. [See Eq. (37) and Fig. 2.] According to Eq. (64), a very rapidly decaying resistive wall mode (on the slowest decaying solution branch) cannot decay faster than

$$-\gamma\,\overline{\tau}_w = \frac{\pi}{2\,\overline{\delta}_w}. \tag{70}$$

Interestingly, rapidly growing resistive wall modes only partially penetrate the wall (in other words, the skin-depth in the wall material is much less than the wall thickness), whereas rapidly decaying modes always penetrate the wall (in other words, the skin-depth in the wall material is of order the wall thickness).

G. Experimental detection of thick-wall effects

Let $\Lambda = -\delta W_{nw}/\delta W_{pw}$. Suppose that we can calculate Λ for two similar plasmas using an ideal-MHD stability code, and can also measure the corresponding growth-rates, γ, of the resistive wall mode experimentally. We can then form the ratio

$$\frac{\gamma_2}{\gamma_1}\,\frac{\Lambda_1}{\Lambda_2} = \sqrt{\frac{\gamma_2}{\gamma_1}}\,\frac{\tanh\left(\sqrt{\gamma_1\,\overline{\delta}_w\,\overline{\tau}_w}\right)}{\tanh\left(\sqrt{\gamma_2\,\overline{\delta}_w\,\overline{\tau}_w}\right)}, \tag{71}$$

where the subscript 1 refers to the first plasma, et cetera. Thick-wall effects would manifest themselves by making this ratio differ from unity. This test becomes more sensitive in the limit in which the ratio γ_1/γ_2 differs substantially from unity.

If the ratio in the previous equation differs from unity then we can use the right-hand side of the equation to estimate $\overline{\delta}_w\,\overline{\tau}_w$. We can then compare one of the growth-rates with Eq. (63) to estimate $\overline{\tau}_w/\overline{\delta}_w$. In this manner, we could estimate both the effective wall thickness parameter, $\overline{\delta}_w$, and the effective wall L/R time, $\overline{\tau}_w$, from experimental data. Note that this estimation method depends on the assumption that the effective minor radius of the wall, $\overline{b}$, is the same in

both plasmas. However, according to Eq. (107), in cylindrical geometry, the ratio of $\overline{b}$ to the actual minor radius of the wall, b, depends on the poloidal and toroidal mode numbers of the resistive wall mode and the minor radius of the plasma, but is otherwise independent of the plasma equilibrium. Hence, the assumption that $\overline{b}/b$ is the same in both plasmas seems reasonable.

H. Further generalization of the Haney–Freidberg formula

Our analysis has assumed that the thickness, d, and conductivity, σ_w, of the wall are uniform. However, if we redo the analysis without making this assumption then very similar arguments reveal that

$$\frac{\int_{S_w}\sqrt{\gamma\,\overline{\tau}_w/\overline{\delta}_w}\tanh\left(\sqrt{\overline{\delta}_w\,\gamma\,\overline{\tau}_w}\right)|\mathbf{A}_{nw}\times\mathbf{n}_w|^2\,dS_w}{\int_{S_w}|\mathbf{A}_{nw}\times\mathbf{n}_w|^2\,dS_w}=-\frac{\delta W_{nw}}{\delta W_{pw}},\quad(72)$$

where both d and σ_w, which appear inside the expressions for $\overline{\tau}_w$ and $\overline{\delta}_w$ [see Eqs. (60) and (61)], are now allowed to vary around the wall.

Note that the previous equation can be reexpressed in the form

$$\gamma\int_{V_w}\sigma_w f(\lambda)\,|\mathbf{A}_{nw}\times\mathbf{n}_w|^2\,dV_w=-\delta W_{nw}\left(1-\frac{\delta W_{nw}}{\delta W_{pw}}\right),\quad(73)$$

where $\lambda=(\gamma\,\mu_0\,\sigma_w\,d^2)^{1/2}$ and $f(x)=(1/2)\tanh(x)/x$. Here, $\mathbf{A}_{nw}$ is evaluated on the inner surface of the wall. This formula is clearly related to the following completely general expression first derived by Pfirsch and Tasso in 1971:[6]

$$\gamma\int_{V_w}\sigma_w\,|\mathbf{A}_w|^2\,dV_w=-\delta W.\quad(74)$$

Here, we have neglected plasma inertia in Pfirsch and Tasso's Eq. (14).

IV. AXISYMMETRIC QUASI-CYLINDRICAL EQUILIBRIUM

A. Introduction

In order to further illustrate some of the arguments presented in this paper, let us calculate the resistive wall stability of an axisymmetric toroidal plasma of major radius R_0 that is modeled as a periodic cylinder.

Let r, θ, z be right-handed cylindrical coordinates. Let the magnetic axis of the plasma corresponds to $r=0$, and let the cylinder be periodic in the z-direction, with periodicity length $2\pi\,R_0$.

B. Plasma equilibrium

The plasma equilibrium is such that $p=p(r)$ and $\mathbf{B}=B_\theta(r)\,\mathbf{e}_\theta+B_z(r)\,\mathbf{e}_z$. Force balance within the plasma yields

$$\mu_0\,p'+B_\theta\,B_\theta'+B_z\,B_z'+\frac{B_\theta^2}{r}=0,\quad(75)$$

where $'\equiv d/dr$. Force balance across the plasma boundary, which lies at $r=a$, demands that

$$2\,\mu_0\,p+B_\theta^2+B_z^2=\hat{B}_\theta^2+\hat{B}_z^2,\quad(76)$$

at $r=a$. In the vacuum region, $r>a$, we have $\hat{B}_\theta'=-\hat{B}_\theta/r$ and $\hat{B}_z'=0$.

C. Perturbation

Let us assume that all perturbed quantities vary with θ and z as $\exp[\mathrm{i}(m\,\theta+k\,z)]$, where m is the poloidal mode number of the instability, $k=n/R_0$, and $n>0$ is the toroidal mode number. The plasma displacement is written $\boldsymbol{\xi}=\boldsymbol{\xi}_\perp+\xi_\parallel\,\mathbf{b}=\xi(r)\,\mathbf{e}_r+\eta(r)\,\mathbf{e}_\eta+\xi_\parallel(r)\,\mathbf{b}$, where $\mathbf{e}_\eta=(B_z/B)\,\mathbf{e}_\theta-(B_\theta/B)\,\mathbf{e}_z$, and $\mathbf{b}=(B_\theta/B)\,\mathbf{e}_\theta+(B_z B)\,\mathbf{e}_z$. Here, ξ is assumed to be real, whereas η and $\xi_\parallel$ turn out to be imaginary. Note that $\mathbf{e}_r$, $\mathbf{e}_\eta$, and $\mathbf{b}$ form a right-handed set of mutually orthogonal unit vectors.

D. Plasma potential energy

In Subsection 7 of the Appendix, it is shown that the minimization of the perturbed plasma potential energy leads to Refs. 9–11 and 21

$$\delta W_p=\frac{\pi^2\,R_0}{\mu_0}\left\{\int_0^a(f\,\xi'^2+g\,\xi^2)\,dr+\left(\frac{k^2\,r^2\,B_z^2-m^2\,B_\theta^2}{k_0^2\,r^2}\right)_a\xi^2(a)\right\},\quad(77)$$

where

$$f(r)=\frac{r\,F^2}{k_0^2},\quad(78)$$

$$g(r)=\frac{2\,k^2}{k_0^2}\,\mu_0\,p'+\left(\frac{k_0^2\,r^2-1}{k_0^2\,r^2}\right)r\,F^2+\frac{2\,k^2}{r\,k_0^4}\left(k\,B_z-\frac{m}{r}\,B_\theta\right)F.\quad(79)$$

Here, $F(r)$ and $k_0(r)$ are defined in Eqs. (A42) and (A43), respectively.

E. Surface potential energy

The perturbed potential energy associated with equilibrium surface currents can easily be shown to take the form

$$\delta W_s=\frac{\pi^2\,R_0}{\mu_0}\,(B_\theta^2-\hat{B}_\theta^2)_a\,\xi^2(a).\quad(80)$$

F. Vacuum region

We shall write the divergence- and curl-free perturbed magnetic field in the vacuum region as

$$\hat{\mathbf{Q}}=\nabla\times\mathbf{A}=\mathrm{i}\,\nabla V.\quad(81)$$

Here, $V=V(r)\,\exp[\mathrm{i}(m\,\theta+k\,z)]$, where $V(r)$ is assumed to be real. Now, the wall matching condition (37) implies that $(m/r)\,A_\theta+k\,A_z=0$. Hence, we deduce that

$$\mathrm{i}\,A_r=-\frac{m\,k}{r^2\,k_0^4}\,\frac{dV}{dr},\quad(82)$$

$$A_\theta=-\frac{k}{k_0^2}\,\frac{dV}{dr},\quad(83)$$

$$A_z=\frac{m}{r\,k_0^2}\,\frac{dV}{dr}.\quad(84)$$

G. Matching conditions at the plasma boundary

Given that $\mathbf{n} = \mathbf{e}_r$, the essential boundary condition (8) yields

$$\hat{F}\,\xi = \frac{dV}{dr}, \tag{85}$$

at $r = a$, where $\hat{F}(r) = (m/r)\,\hat{B}_\theta + k\,\hat{B}_z$. Moreover, the pressure balance matching condition, (9), reduces to

$$f\,\xi' + \left(\frac{k^2\,r^2\,B_z^2 - m^2\,B_\theta^2}{k_0^2\,r^2}\right)\xi + (B_\theta^2 - \hat{B}_\theta^2)\,\xi = r\,\hat{F}\,V, \tag{86}$$

at $r = a$.

H. Matching conditions at wall

The wall is assumed to be uniform, and located at minor radius $r = b$. Given that $\mathbf{n}_w = \mathbf{e}_r$, the essential boundary condition (37) gives

$$\left(\frac{dV}{dr}\right)_{b_-} = \cosh\lambda\left(\frac{dV}{dr}\right)_{b_+}. \tag{87}$$

Moreover, the natural boundary condition (38) reduces to

$$V(b_-) + \frac{\lambda\tanh\lambda}{d}\,\frac{1}{k_b^2}\,\frac{dV(b_-)}{dr} = \frac{V(b_+)}{\cosh\lambda}. \tag{88}$$

Here, b_- and b_+ denote the inner and outer wall radii, respectively, where it is assumed that the wall is radially thin. Furthermore, $k_b^2 = m^2/b^2 + k^2$.

I. Vacuum potential energy

The contribution of the vacuum region lying internal to the wall to the overall potential energy of the perturbation can be shown to be [see Eqs. (42) and (81)]

$$\delta W_v^{(i)} = \frac{\pi^2\,R_0}{\mu_0}\left[-\int_a^{b_-} V\,\nabla^2 V\,r\,dr - (r\,\hat{F}\,\xi\,V)_a + \left(r\,\frac{dV}{dr}\,V\right)_{b_-}\right], \tag{89}$$

where use has been made of the essential boundary condition (85). Similarly, the contribution of the vacuum region lying outside the wall is [see Eqs. (43) and (81)]

$$\delta W_v^{(o)} = \frac{\pi^2\,R_0}{\mu_0}\left[-\left(r\,\frac{dV}{dr}\,V\right)_{b_+} - \int_{b_+}^{\infty} V\,\nabla^2 V\,r\,dr\right]. \tag{90}$$

J. Wall potential energy

The contribution of the wall to the overall potential energy of the perturbation can be shown to take the form [see Eqs. (44), (83), and (84)]

$$\delta W_v^{(w)} = \frac{\pi^2\,R_0}{\mu_0}\,\frac{\lambda\tanh\lambda}{d}\,\frac{b}{k_b^2}\left(\frac{dV}{dr}\right)_{b_-}^2. \tag{91}$$

K. Variation principle

In Subsection 8 of the Appendix, we demonstrate that the perturbation that minimizes the total perturbed potential energy, $\delta W = \delta W_p + \delta W_s + \delta W_v^{(i)} + \delta W_w + \delta W_v^{(o)}$, satisfies *Newcomb's equation*,[21]

$$(f\,\xi')' - g\,\xi = 0, \tag{92}$$

in the plasma, satisfies

$$\nabla^2 V \equiv \frac{1}{r}\,\frac{d}{dr}\left(r\,\frac{dV}{dr}\right) - \left(\frac{m^2}{r^2} + k^2\right)V = 0, \tag{93}$$

in the vacuum, and satisfies the natural boundary conditions (86) and (88) at the plasma boundary and at the wall, respectively.

L. No-wall and perfect-wall energies

The independent solutions of Eq. (93) are $I_{|m|}(k\,r)$ and $K_{|m|}(k\,r)$, where $I_m(z)$ and $K_m(z)$ are modified Bessel functions. The vacuum scalar potential associated with the no-wall solution must satisfy

$$\frac{dV_{nw}}{dr} = \hat{F}(a)\,\xi(a) \tag{94}$$

at the plasma boundary [see Eq. (85)], and

$$V_{nw} = 0 \tag{95}$$

at infinity [see Eq. (A18)]. It follows that

$$V_{nw}(r) = \frac{\hat{F}(a)\,\xi(a)}{k}\,\frac{K_{|m|}(k\,r)}{K'_{|m|}(k\,a)}. \tag{96}$$

Here, $'$ denotes differentiation with respect to argument. The vacuum potential energy associated with the no-wall solution is

$$\delta W_v^{(\infty)} = -\frac{\pi^2\,R_0}{\mu_0}\,(r\,\hat{F}\,\xi\,V_{nw})_a, \tag{97}$$

where use has been made of Eqs. (42), (81), (85), (93), and (95).

The vacuum scalar potential associated with the perfect-wall solution must satisfy

$$\frac{dV_{pw}}{dr} = \hat{F}(a)\,\xi(a) \tag{98}$$

at the plasma boundary [see Eq. (85)], and

$$\frac{dV_{pw}}{dr} = 0 \tag{99}$$

at the wall [see Eq. (A14)]. It follows that

$$V_{pw}(r) = \frac{\hat{F}(a)\,\xi(a)}{k}\,\frac{I_{|m|}(k\,r)\,K'_{|m|}(k\,b) - K_{|m|}(k\,r)\,I'_{|m|}(k\,b)}{I'_{|m|}(k\,a)\,K'_{|m|}(k\,b) - K'_{|m|}(k\,a)\,I'_{|m|}(k\,b)}. \tag{100}$$

The vacuum potential energy associated with the perfect-wall solution is

$$\delta W_v^{(b)} = -\frac{\pi^2\,R_0}{\mu_0}\,(r\,\hat{F}\,\xi\,V_{pw})_a, \tag{101}$$

where use has been made of Eqs. (42), (81), (85), (93), and (99).

Now, integrating by parts, and making use of Eq. (92), the expression, (77), for the plasma potential energy becomes

$$\delta W_p = \frac{\pi^2 R_0}{\mu_0}\left\{\xi\left[f\,\xi' + \left(\frac{k^2 r^2 B_z^2 - m^2 B_\theta^2}{k_0^2 r^2}\right)\xi\right]\right\}_a. \tag{102}$$

Thus, the total potential energy of the no-wall ideal external-kink mode takes the form

$$\begin{aligned}\delta W_{nw} &= \delta W_p + \delta W_s + \delta W_v^{(\infty)}\\ &= \frac{\pi^2 R_0}{\mu_0}\left\{\xi\left[f\,\xi' + \left(\frac{k^2 r^2 B_z^2 - m^2 B_\theta^2}{k_0^2 r^2}\right)\xi\right.\right.\\ &\left.\left. + (B_\theta^2 - \hat{B}_\theta^2)\,\xi - r\hat{F}\,V_{nw}\right]\right\}_a.\end{aligned} \tag{103}$$

Likewise, the total potential energy of the perfect-wall ideal external-kink mode can be written as

$$\begin{aligned}\delta W_{pw} &= \delta W_p + \delta W_s + \delta W_v^{(b)}\\ &= \frac{\pi^2 R_0}{\mu_0}\left\{\xi\left[f\,\xi' + \left(\frac{k^2 r^2 B_z^2 - m^2 B_\theta^2}{k_0^2 r^2}\right)\xi\right.\right.\\ &\left.\left. + (B_\theta^2 - \hat{B}_\theta^2)\,\xi - r\hat{F}\,V_{pw}\right]\right\}_a.\end{aligned} \tag{104}$$

In accordance with the discussion in Sec. II G, we can see that the only reason that the energies δW_{nw} and δW_{pw} can take non-zero values is because the solution pairs, $[\xi(r), V(r)]$, from which they are constructed, do not satisfy the pressure balance matching condition, (86), at the plasma boundary.

M. Effective wall radius

It follows from Eqs. (96), (97), (100), and (101) that

$$\begin{aligned}&\delta W_v^{(b)} - \delta W_v^{(\infty)}\\ &= \frac{\pi^2 R_0}{\mu_0}\frac{(r\hat{F}\,\xi)_a^2\,K'_{|m|}(k\,b)}{(k\,a)^2\,K'_{|m|}(k\,a)\left[I'_{|m|}(k\,a)\,K'_{|m|}(k\,b) - K'_{|m|}(k\,a)\,I'_{|m|}(k\,b)\right]}.\end{aligned} \tag{105}$$

Moreover,

$$\begin{aligned}&\frac{1}{2\,\mu_0}\int_{S_w}|\mathbf{A}_{nw}\times\mathbf{e}_r|^2\,dS_w\\ &= \frac{\pi^2 R_0}{\mu_0}\frac{b}{k_b^2}\left(\frac{dV_{nw}}{dr}\right)_b^2\\ &= \frac{\pi^2 R_0}{\mu_0}\,(r\hat{F}\,\xi)_a^2\,\frac{b}{(k_b\,a)^2}\left[\frac{K'_{|m|}(k\,b)}{K'_{|m|}(k\,a)}\right]^2,\end{aligned} \tag{106}$$

where use has been made of Eqs. (83), (84), and (96). Hence, it follows from Eq. (57) that the ratio of the effective wall minor radius to the actual wall minor radius is[10]

$$\frac{\overline{b}}{b} = \frac{(k\,b)^2}{m^2 + (k\,b)^2}\frac{K'_{|m|}(k\,b)}{K'_{|m|}(k\,a)}\left[I'_{|m|}(k\,a)\,K'_{|m|}(k\,b) - K'_{|m|}(k\,a)\,I'_{|m|}(k\,b)\right]. \tag{107}$$

N. Pressure balance matching condition

Let

$$P_a = \left[f\,\xi' + \left(\frac{k^2 r^2 B_z^2 - m^2 B_\theta^2}{k_0^2 r^2}\right)\xi + (B_\theta^2 - \hat{B}_\theta^2)\,\xi\right]_a. \tag{108}$$

According to Eqs. (67), (68), (103), and (104),

$$c_1 = \frac{\left[P_a - (r\hat{F}\,V_{pw})_a\right]}{\left[r\hat{F}\,(V_{nw} - V_{pw})\right]_a}, \tag{109}$$

$$c_2 = -\frac{\left[P_a - (r\hat{F}\,V_{nw})_a\right]}{\left[r\hat{F}\,(V_{nw} - V_{pw})\right]_a}. \tag{110}$$

Thus, the linear combination of solutions that satisfies the resistive wall mode problem is characterized by [see Eq. (47)]

$$(r\hat{F}\,V)_a = c_1\,(r\hat{F}\,V_{nw})_a + c_2\,(r\hat{F}\,V_{pw})_a = P_a. \tag{111}$$

However, the pressure balance matching condition at the plasma boundary, (86), can be written as

$$P_a = (r\hat{F}\,V)_a. \tag{112}$$

Thus, it is clear, from a comparison of the previous two equations, that the matching condition is satisfied.

The natural boundary condition at the wall, (88), is satisfied when the growth-rate of the resistive wall mode takes the value [see Eqs. (60), (61), (63), and (64)]

$$\sqrt{\frac{\gamma\,\tau_w}{\delta_w}}\tanh\left(\sqrt{\delta_w\,\gamma\,\tau_w}\right) = -\frac{b}{\overline{b}}\frac{\delta W_{nw}}{\delta W_{pw}}. \tag{113}$$

Here, $\tau_w = \mu_0\,\sigma_w\,d\,b$ is the true time-constant of the wall, and $\delta_w = d/b$ is a measure of its true thickness.

O. Force-free reversed-field pinch equilibrium

Consider a reversed-field pinch[10] plasma equilibrium. Let us assume, for the sake of simplicity, that the equilibrium pressure is negligible. In this case, the equilibrium magnetic field, both in the plasma and in the vacuum, satisfies[22]

$$B'_\theta = \sigma\,B_z - \frac{B_\theta}{r}, \tag{114}$$

$$B'_z = -\sigma\,B_\theta, \tag{115}$$

where $\sigma(r) = \mu_0\,\mathbf{j}\cdot\mathbf{B}/B^2$. Let us adopt the following model $\sigma(r)$ profile,[22]

$$\sigma(r) = \begin{cases}\sigma_0\left[1 - (r/a)^\alpha\right]^\nu, & r \le a,\\ 0, & r > a,\end{cases} \tag{116}$$

where α, $\nu > 0$. Note that $\sigma(a) = 0$, which implies that there is no equilibrium current sheet flowing around the plasma boundary.

The resistive wall mode perturbation can be specified, both in the plasma and in the vacuum, in terms of the perturbed poloidal flux, $\psi(r)$,[5] where

$$\psi(r) = \begin{cases} r\,F\,\xi, & r \le a, \\ r\,(dV/dr), & r > a. \end{cases} \tag{117}$$

The matching condition (85) becomes

$$\psi(a_-) = \psi(a_+), \tag{118}$$

whereas the pressure balance matching condition, (86), reduces to

$$r\,\frac{d\psi}{dr}\bigg|_{a_-} = r\,\frac{d\psi}{dr}\bigg|_{a_+}. \tag{119}$$

Note that a failure to satisfy the pressure balance matching condition is associated with a gradient discontinuity in $\psi(r)$ at the plasma boundary. Such a discontinuity implies the existence of a perturbed current sheet flowing on the boundary.

Inside the plasma, Newcomb's equation, (92), can be re-expressed in the form[22]

$$(\hat{f}\,\psi')' - \hat{g}\,\psi = 0, \tag{120}$$

where

$$\hat{f}(r) = \frac{1}{r\,k_0^2}, \tag{121}$$

$$\hat{g}(r) = \frac{1}{r} + \frac{\sigma'\,G}{r\,k_0^2\,F} - \frac{2\,m\,k\,\sigma}{r^3\,k_0^4} - \frac{\sigma^2}{r\,k_0^2}. \tag{122}$$

Here, $G(r)$ is defined in Eq. (A41). Note that Eq. (120) is singular at any equilibrium magnetic flux-surface, $r = r_s$, lying within the plasma, that satisfies $F(r_s) = 0$. An ideal solution (which is unable to reconnect magnetic field-lines) must satisfy $\psi(r_s) = 0$ at such a surface.[5,10] It is helpful to define

$$c_p = \left(r\,\frac{d\psi_p}{dr}\right)_a, \tag{123}$$

where $\psi_p(r)$ is a solution of Eq. (120) that is well-behaved at $r = 0$, satisfies $\psi(r_s) = 0$ at any singular surfaces within the plasma, and is such that $\psi_p(a) = 1$. Thus, the solution in the region $0 \le r \le a$ becomes

$$\psi(r) = \psi_a\,\psi_p(r), \tag{124}$$

where $\psi_a = \psi(a)$, which is the value of the perturbed poloidal magnetic flux at the plasma boundary, is undetermined.Outside the plasma, in the region $r > a$, we can write

$$\psi(r) = \psi_a\,\psi_{rwm}(r) = \psi_a\,[c_1\,\psi_{nw}(r) + c_2\,\psi_{pw}(r)], \tag{125}$$

where $\psi_{nw}(a) = \psi_{pw}(a) = 1$, and $c_1 + c_2 = 1$. [See Eqs. (132) and (133).] This automatically satisfies the matching condition (120). Here,

$$\psi_{nw}(r) = \frac{r}{a}\,\frac{K'_{|m|}(k\,r)}{K'_{|m|}(k\,a)}, \tag{126}$$

$$\psi_{pw}(r) = \frac{r}{a}\,\frac{I'_{|m|}(k\,r)\,K'_{|m|}(k\,b) - K'_{|m|}(k\,r)\,I'_{|m|}(k\,b)}{I'_{|m|}(k\,a)\,K'_{|m|}(k\,b) - K'_{|m|}(k\,a)\,I'_{|m|}(k\,b)}. \tag{127}$$

Note that $\psi_{nw}(\infty) = \psi_{pw}(b) = 0$, in accordance with Eqs. (95) and (99). Furthermore, it is understood that $\psi_{pw}(r > b) = 0$. It is helpful to define

$$c_{nw} = \left(r\,\frac{d\psi_{nw}}{dr}\right)_a = \frac{m^2 + (k\,a)^2}{k\,a}\,\frac{K_{|m|}(k\,a)}{K'_{|m|}(k\,a)}, \tag{128}$$

$$c_{pw} = \left(r\,\frac{d\psi_{pw}}{dr}\right)_a = \frac{m^2 + (k\,a)^2}{k\,a}\,\frac{I_{|m|}(k\,a)\,K'_{|m|}(k\,b) - K_{|m|}(k\,a)\,I'_{|m|}(k\,b)}{I'_{|m|}(k\,a)\,K'_{|m|}(k\,b) - K'_{|m|}(k\,a)\,I'_{|m|}(k\,b)}. \tag{129}$$

It is easily demonstrated that

$$\delta W_{nw} = \frac{\pi^2\,R_0}{\mu_0}\,\frac{\psi_a^2}{m^2 + (k\,a)^2}\,(c_p - c_{nw}), \tag{130}$$

$$\delta W_{pw} = \frac{\pi^2\,R_0}{\mu_0}\,\frac{\psi_a^2}{m^2 + (k\,a)^2}\,(c_p - c_{pw}). \tag{131}$$

Furthermore,

$$c_1 = \frac{c_p - c_{pw}}{c_{nw} - c_{pw}}, \tag{132}$$

$$c_2 = \frac{c_{nw} - c_p}{c_{nw} - c_{pw}}. \tag{133}$$

Note that $c_1 + c_2 = 1$.

The resistive wall dispersion relation, (113), becomes

$$\sqrt{\frac{\gamma\,\tau_w}{\delta_w}}\tanh\sqrt{\delta_w\,\gamma\,\tau_w} = c_b\left(\frac{c_{nw} - c_p}{c_p - c_{pw}}\right), \tag{134}$$

where

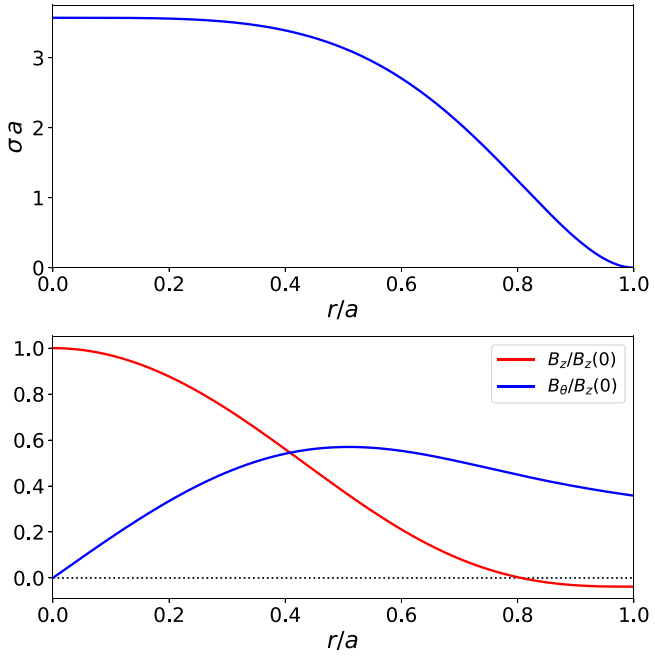

FIG. 4. Force-free reversed-field pinch equilibrium characterized by $a/R_0 = 0.25$, $\sigma_0\,a = 3.57$, $\alpha = 4.0$, and $\nu = 2.0$.

$$c_b = \frac{(k\,b)^2}{m^2 + (k\,b)^2}\,\frac{K'_{|m|}(k\,b)}{K'_{|m|}(k\,a)}\left[I'_{|m|}(k\,a)\,K'_{|m|}(k\,b) - K'_{|m|}(k\,a)\,I'_{|m|}(k\,b)\right]. \tag{135}$$

Thus, the whole problem is fully specified, for given poloidal and toroidal mode numbers, once the parameter c_p, defined in Eq. (123), is numerically calculated from the modified Newcomb equation, (120).

P. Example calculation

Let us adopt the following equilibrium parameters: $a/R_0 = 0.25$, $\sigma_0\,a = 3.57$, $\alpha = 4.0$, and $\nu = 2.0$. The resulting generic reversed-field pinch equilibrium is shown in Fig. 4. The characteristic pinch and reversal parameters[10] are $\Theta = 1.70$ and $F = -0.18$, respectively. As is well-known, it is necessary to place the wall relatively close to a reversed-field pinch plasma in order to stabilize all possible ideal external-kink modes.[10] In the present case, we choose $b/a = 1.12$. The thickness of the wall is $d/a = 0.4$, which is the largest value that we could adopt and plausibly argue that $d/b \ll 1$.

Consider the $m = -1/n = 11$ resistive wall mode. This is a mode that possesses a resonant surface in the plasma located at $r/a = 0.463$. The no-wall and perfect-wall energies of the mode are $\delta W_{nw} = 0.359\,(\pi^2\,R_0\,\psi_a^2/\mu_0)$ and $\delta W_{pw} = 1.030\,(\pi^2\,R_0\,\psi_a^2/\mu_0)$, respectively. The fact that both energies are positive indicates that the mode is stable. In fact, the decay-rate of the mode is $-\gamma\,\tau_w = 0.026\,77$. If the wall were in the thin-shell limit, but had the same τ_w value, then the decay-rate would have been $-\gamma\tau_w = 0.026\,85$. Thus, the finite thickness of the wall has decreased the decay-rate of mode, in accordance with the discussion in Sec. III F. However, despite the comparatively large wall thickness, the reduction is extremely modest.

Figure 5 shows the eigenfunctions of the $m = -1/n = 11$ resistive wall mode. The no-wall ideal external-kink mode has the eigenfunction $[\psi_p(r),\,\psi_{nw}(r)]$, where the first function corresponds to the plasma, whereas the second corresponds to the vacuum. It can be seen that this eigenfunction has a gradient discontinuity at the plasma boundary, indicating that it does not satisfy the pressure balance matching condition. The perfect-wall ideal external-kink mode has the eigenfunction $[\psi_p(r),\,\psi_{pw}(r)]$. Again, this eigenfunction has a gradient discontinuity at the plasma boundary, indicating that it does not satisfy the pressure balance matching condition. Finally, the resistive wall mode has the eigenfunction $[\psi_p(r),\,\psi_{rwm}(r)]$. Note that this eigenfunction is completely continuous across the plasma boundary, indicating that it does satisfy the pressure balance matching condition.

Figure 6 shows the growth-rates of the $m = -1$, $m = 0$, and $m = 1$ resistive wall modes, calculated for n in the range 1–20, and for various values of the wall thickness. It can be seen that the varying wall thickness makes no discernible difference to the growth-rates of the modes, with the exception of the $m = -1/n = 7$ mode. It turns out that the $m = -1/n = 7$ ideal external-kink mode is barely stabilized by a perfectly-conducting wall located at $b/a = 1.12$. Consequently, the corresponding resistive wall mode has a comparatively large growth-rate. In fact, in this case, it can be seen that increasing wall thickness (at fixed τ_w) leads to a noticeable increase in the growth-rate, in accordance with the discussion in Sec. III F. Thus, we conclude that thick-wall effects are only important for resistive wall modes that lie fairly close to the perfect-wall ideal stability boundary.

V. ROTATIONAL STABILIZATION OF THE RESISTIVE WALL MODE

A. Generalized Hu-Betti formula

So far, the analysis presented this paper suggests that the marginal stability point for the resistive wall mode is the same as that for the no-wall ideal external-kink mode: i.e., $\delta W_{pw} = 0$.[6] In other words, a close-

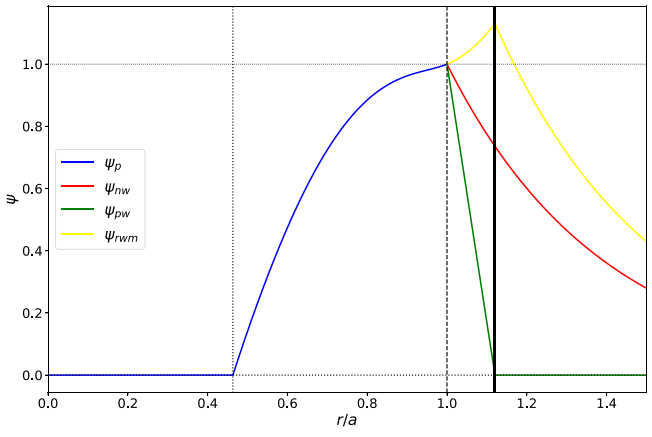

FIG. 5. Eigenfunctions of an $m = -1/n = 11$ resistive wall mode in a force-free reversed-field pinch equilibrium characterized by $a/R_0 = 0.25$, $\sigma_0\,a = 3.57$, $\alpha = 4.0$, $\nu = 2.0$, $b/a = 1.12$, and $d/a = 0.4$. The dotted vertical line indicates the resonant surface, the dashed vertical line indicates the plasma boundary, and the solid vertical line indicates the inner surface of the wall.

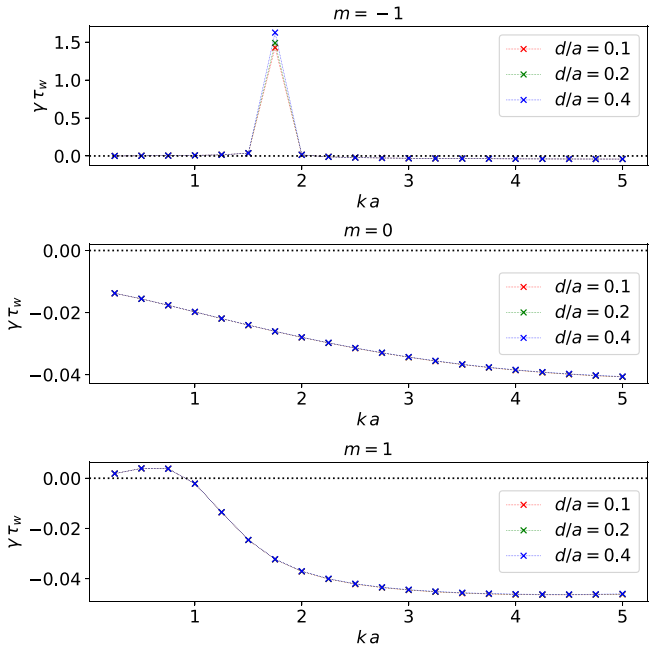

FIG. 6. Growth-rates of $m = -1$, $m = 0$, and $m = 1$ resistive wall modes calculated in a force-free reversed-field pinch equilibrium characterized by $a/R_0 = 0.25$, $\sigma_0\,a = 3.57$, $\alpha = 4.0$, $\nu = 2.0$, and $b/a = 1.12$, for various values of the wall thickness. Note that most of the data points for different wall thicknesses plot on top of one another.

fitting resistive wall is capable of transforming a rapidly growing ideal external-kink mode into a slowly growing resistive wall mode, but is unable to completely stabilize the mode.[6,10] This conclusion is ultimately a consequence of the fact that the plasma potential energy, δW_p, is a real quantity. However, it turns out that resonances within the plasma, in combination with toroidal plasma rotation, allow δW_p to acquire an imaginary component.[23] The resonances in question include resonances with the sound wave continuum,[24] resonances with the shear-Alfvén wave continuum,[25] and resonances with trapped and circulating particles.[26,27] Furthermore, above a critical plasma rotation rate, the resistive wall mode is stabilized by the imaginary component of δW_p.[28]

Let us write $\delta W_p = \delta W_p^{(r)} + \mathrm{i}\,\delta W_p^{(i)}$, where $\delta W_p^{(r)}$ and $\delta W_p^{(i)}$ are the real and imaginary components of δW_p, respectively. We can then make the following redefinitions:

$$\delta W_{pw} = \delta W_p^{(r)} + \delta W_s + \delta W_v^{(b)}, \tag{136}$$

$$\delta W_{nw} = \delta W_p^{(r)} + \delta W_s + \delta W_v^{(\infty)}. \tag{137}$$

Incidentally, it is obvious, from their definitions, that δW_s, $\delta W_v^{(b)}$, and $\delta W_v^{(\infty)}$ are all real quantities. Note that the real part of the resonant contribution to δW_p has been incorporated into $\delta W_p^{(r)}$. In general, we expect $\delta W_p^{(i)}$ to be proportional to the toroidal plasma rotation at the resonant point within the plasma.[24]

In the presence of resonances, our generalized Haney–Freidberg formula, (63), generalizes further to give

$$\sqrt{\frac{\gamma\,\overline{\tau}_w}{\overline{\delta}_w}}\tanh\left(\sqrt{\overline{\delta}_w\,\gamma\,\overline{\tau}_w}\right) = -\left(\frac{\delta W_{nw} + \mathrm{i}\,\delta W_p^{(i)}}{\delta W_{pw} + \mathrm{i}\,\delta W_p^{(i)}}\right), \tag{138}$$

where $\gamma = \gamma_r - \mathrm{i}\,\omega_r$. Here, γ_r and ω_r are the real growth-rate and real frequency of the resistive wall mode, respectively. The previous formula is a generalization of a formula that first appeared in a paper by Hu and Betti in 2004.[26]

Note, incidentally, that it is not obvious that the force operator, $\mathbf{F}(\boldsymbol{\xi})$, remains self-adjoint in the presence of an imaginary resonant contribution to δW_p. Given that the proof of the variation principle, upon which Eq. (63) is based, is itself based on the self-adjoint nature of the force operator, this calls into question the validity of the Hu and Betti formula, and the previous generalization. However, in the following, we shall assume that these formulas are correct.

B. Marginal stability point

Let us assume that the resistive wall mode is unstable in the absence of an imaginary resonant contribution to δW_p, which implies that $\delta W_{nw} < 0$ and $\delta W_{pw} > 0$. Let us search for a marginal stability point at which $\gamma_r = 0$. If we define $x = \omega_r\,\overline{\tau}_w$, $y = \delta W_p^{(i)}/\delta W_{pw}$, $z = -\delta W_{nw}/\delta W_{pw}$, $\zeta = [x/(2\,\overline{\delta}_w)]^{1/2}$, $\mu = (2\,\overline{\delta}_w\,x)^{1/2}$, $S = \sinh\mu$, $C = \cosh\mu$, $s = \sin\mu$, $c = \cos\mu$, and

$$\alpha(x) = \zeta\left(\frac{S-s}{C+c}\right), \tag{139}$$

$$\beta(x) = \zeta\left(\frac{S+s}{C+c}\right), \tag{140}$$

then Eq. (138) yields

$$\alpha = \frac{z-y^2}{1+y^2}, \tag{141}$$

$$\beta = \frac{y\,(1+z)}{1+y^2}. \tag{142}$$

Here, we are assuming, without loss of generality, that $x > 0$ and $y > 0$. This assumption simply implies an arbitrary choice of the direction of plasma rotation. The previous two equations can be combined to give

$$F(x) \equiv \beta^2 - (z-\alpha)\,(1+\alpha) = 0. \tag{143}$$

Once x has been determined, by finding the root of the previous equation, y is specified by

$$y = \sqrt{\frac{z-\alpha}{1+\alpha}}. \tag{144}$$

Figure 7 shows the critical real frequency, ω_r, and the critical imaginary part of the plasma potential energy, $\delta W_p^{(i)}$, needed to stabilize the resistive wall mode, according to the generalized Hu–Betti formula, (138). It can be seen that increasing wall thickness (at fixed $\overline{\tau}_w$) facilitates the stabilization of the resistive wall mode, because it decreases the critical value of $\delta W_p^{(i)}$, which corresponds to a decreased critical plasma rotational rate. On the other hand, the real frequency of the mode at the marginal stability point increases with increasing wall thickness. Note, finally, that the thick-wall stabilization criterion only differs substantially from the thin-wall stabilization criterion, which is

$$(\omega_r\,\overline{\tau}_w)_{crit} = \left[\frac{\delta W_p^{(i)}}{\delta W_{pw}}\right]_{crit} = \sqrt{-\frac{\delta W_{nw}}{\delta W_{pw}}}, \tag{145}$$

when $-\delta W_{nw}/\delta W_{pw} \gtrsim 1$, which implies that the corresponding external-kink mode lies fairly close to the perfect-wall stability boundary.

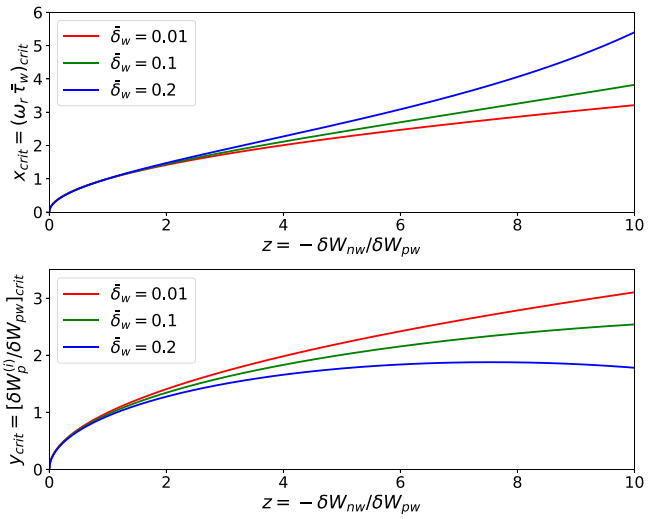

FIG. 7. Critical real frequency, ω_r, and critical imaginary part of the plasma potential energy, $\delta W_p^{(i)}$, needed to stabilize the resistive wall mode according to the generalized Hu–Betti formula, (138).

C. Toroidal electromagnetic torque

As pointed out by Park,[29] there is an intimate connection between the imaginary component of the plasma potential energy, $\delta W_p^{(i)}$, and the net toroidal electromagnetic torque exerted by the resistive wall on the plasma. Let us investigate this connection.

Employing the cylindrical analysis of Sec. IV, the net outward flux of toroidal angular momentum across a magnetic flux-surface of minor radius r, lying outside the plasma, is[30]

$$T_\phi(r) = \frac{1}{2\,\mu_0}\oint\int_0^{2\pi R_0} r\,R_0\left(\hat{Q}_z^*\,\hat{Q}_r + \hat{Q}_z\,\hat{Q}_r^*\right) d\theta\,dz. \tag{146}$$

Given that $\hat{\mathbf{Q}} = \mathrm{i}\,\nabla V$ in a vacuum region, we deduce that

$$T_\phi(r) = \frac{\pi^2\,n\,R_0}{\mu_0}\,\mathrm{i}\left(-V^*\,r\,\frac{dV}{dr} + V\,r\,\frac{dV^*}{dr}\right), \tag{147}$$

where the additional factor of 1/2 comes from averaging $\cos^2(m\,\theta + k\,z)$, and $n = k\,R$ is the toroidal mode number. However, it is clear from Eq. (93) that

$$\frac{d}{dr}\left(V^*\,r\,\frac{dV}{dr} - V\,r\,\frac{dV^*}{dr}\right) = 0. \tag{148}$$

Hence, we conclude that

$$\frac{dT_\phi}{dr} = 0. \tag{149}$$

in any vacuum region.[31]

Now, in the vacuum region beyond the wall,

$$V(r) = \psi_a\,c_3\,\hat{V}_{nw}(r) \tag{150}$$

[see Eq. (48)], where $\psi_a = (r\,\hat{F}\,\xi)_a$ is the value of the perturbed poloidal magnetic flux at the plasma boundary, and

$$\hat{V}_{nw}(r) = \frac{1}{k\,a}\,\frac{K_{|m|}(k\,r)}{K_{|m|'}(k\,a)}. \tag{151}$$

[See Eq. (96).] However, it is obvious from Eqs. (147) and (150) that

$$T_\phi(r > b) = 0. \tag{152}$$

In other words, the net flux of toroidal angular momentum from the plasma-wall system is zero.

Now, in the vacuum region between the plasma and the wall,

$$V(r) = \psi_a\left[c_1\,\hat{V}_{nw}(r) + c_2\,\hat{V}_{pw}(r)\right] \tag{153}$$

[see Eq. (47)], where $c_1 + c_2 = 0$ [see Eq. (50)]. Here,

$$\hat{V}_{pw}(r) = \frac{1}{k\,a}\,\frac{I_{|m|}(k\,r)\,K'_{|m|}(k\,b) - K_{|m|}(k\,r)\,I'_{|m|}(k\,b)}{I'_{|m|}(k\,a)\,K'_{|m|}(k\,b) - K'_{|m|}(k\,a)\,I'_{|m|}(k\,b)}. \tag{154}$$

[See Eq. (100).] Note that

$$\left(r\,\frac{d\hat{V}_{nw}}{dr}\right)_a = \left(r\,\frac{d\hat{V}_{pw}}{dr}\right)_a = 1. \tag{155}$$

It follows from Eqs. (147) and (153) that

$$T_\phi(a) = -\frac{2\pi^2\,R_0\,n\,\psi_a^2}{\mu_0}\,(\hat{V}_{nw} - \hat{V}_{pm})_a\,\mathrm{Im}(c_1). \tag{156}$$

Thus, if c_1 possesses an imaginary component then there is a constant flux of toroidal electromagnetic angular momentum between the plasma and the wall. This flux is associated with a toroidal electromagnetic torque exerted on the plasma, and an equal and opposite torque exerted on the wall.

Now, according to Eqs. (80), (97), (102), (108), and (109),

$$c_1 = \frac{\mu_0}{\pi^2\,R_0\,\psi_a^2}\,\frac{\delta W_p + \delta W_s + \delta W_v^{(\infty)}}{(\hat{V}_{nw} - \hat{V}_{pw})_a}, \tag{157}$$

which implies that

$$\mathrm{Im}(c_1) = \frac{\mu_0}{\pi^2\,R_0\,\psi_a^2}\,\frac{\mathrm{Im}(\delta W_p)}{(\hat{V}_{nw} - \hat{V}_{pw})_a} = \frac{\mu_0}{\pi^2\,R_0\,\psi_a^2}\,\frac{\delta W_p^{(i)}}{(\hat{V}_{nw} - \hat{V}_{pw})_a}. \tag{158}$$

Here, we have made use of the fact that δW_s and $\delta W_v^{(\infty)}$ are obviously real quantities. Hence, we deduce from Eq. (156) that[29]

$$T_\phi = -2\,n\,\delta W_p^{(i)}. \tag{159}$$

[Note that the opposite sign with respect to the result in Ref. 29 is due to the assumed $\exp(-\mathrm{i}\,n\,z/R_0)$ variation of perturbed quantities in this reference, as opposed to the assumed $\exp(+\mathrm{i}\,n\,z/R_0)$ variation in this paper.] Here, T_ϕ is the toroidal electromagnetic torque acting on the plasma. It follows that the variable y, appearing in the analysis of Sec. V B, represents a normalized electromagnetic torque exerted by the wall on the plasma. In fact,

$$y = -\frac{T_\phi}{2\,n\,\delta W_{pw}}. \tag{160}$$

Thus, we can reinterpret Fig. 7 as stating, first, that the rotational stabilization of the resistive wall mode requires the assistance of such a torque, and, second, that the critical torque needed to stabilize the mode decreases with increasing wall thickness (at constant τ_w).

VI. SUMMARY

This paper investigates the external-kink stability of a toroidal plasma surrounded by a rigid resistive wall. The main aim of this paper is to extend the well-known analysis of Haney and Freidberg[12] to allow for a wall that is sufficiently thick that the thin-shell approximation does not necessarily hold.

In Subsection 4 of the Appendix, we demonstrate that the MHD force operator remains self-adjoint in the presence of a thick resistive wall. In Sec. III C, making use of the self-adjoint property, we modify the variational principle of Haney and Freidberg to allow for a thick wall. Finally, in Sec. III D, we minimize the plasma potential energy to obtain a generalized Haney–Freidberg formula, (63) and (64), for the growth-rate of the resistive wall mode that allows the wall to lie either in the thin-shell regime, the thick-shell regime, or somewhere in between.

We find that thick-wall effects do not change the marginal stability point of the mode,[6] but introduce an interesting asymmetry between growing and decaying modes. Growing modes have growth-rates that exceed those predicted by the original Haney–Freidberg

formula. (Here, we are comparing walls with differing thicknesses but the same L/R time.) On the other hand, decaying modes have decay-rates that are less than those predicted by the original formula. We can even generalize the Haney–Freidberg formula to allow for walls with varying thickness and electrical conductivity. [See Eq. (72).]

We also show, during the course of our investigation, that the eigenfunctions conventionally used to calculate the quantities δW_{nw} and δW_{pw}, that feature in the Haney–Freidberg formula, do not satisfy the pressure balance matching condition at the plasma boundary. We then explain why this is not problematic. In particular, the resistive wall mode eigenfunction is found to satisfy the pressure balance matching condition.

In Sec. IV, we perform a cylindrical calculation for a generic force-free reversed-field pinch plasma equilibrium that reveals that thick-wall effects have no noticeable effect on the growth-rates of the various resistive wall modes to which the plasma is subject, except when the mode in question lies quite close to the perfect-wall stability boundary. For such a comparatively rapidly growing mode, thick-wall effects perceptibly increase the growth-rate.

Finally, in Sec. V, we generalize the well-known Hu–Betti formula[26] for the rotational stabilization of the resistive wall mode to take thick-wall effects into account. We find that increasing wall thickness (at fixed L/R time) facilitates the rotational stabilization of the resistive wall mode, because it decreases the critical toroidal electromagnetic torque that the wall must exert on the plasma. On the other hand, the real frequency of the mode at the marginal stability point increases with increasing wall thickness.

ACKNOWLEDGMENTS

This research was directly funded by the U.S. Department of Energy, Office of Science, Office of Fusion Energy Sciences, under Contract No. DE-SC0021156.

AUTHOR DECLARATIONS

Conflict of Interest

The author has no conflicts to disclose.

Author Contributions

Richard Fitzpatrick: Conceptualization (equal); Formal analysis (equal); Writing – original draft (equal).

DATA AVAILABILITY

The data that support the findings of this study are available from the corresponding author upon reasonable request.

APPENDIX: TECHNICAL DETAILS

1. Self-adjoint property of force operator

Let $[\boldsymbol{\xi}(\mathbf{r}), \mathbf{A}(\mathbf{r})]$ and $[\boldsymbol{\eta}(\mathbf{r}), \mathbf{C}(\mathbf{r})]$ be two independent prospective solution pairs that satisfy both the essential and the natural boundary conditions. It is easily demonstrated that[11]

$$\int_{V_p} \boldsymbol{\eta}\cdot\mathbf{F}(\boldsymbol{\xi})\,dV_p = -\int_{V_p}\Big[\Gamma\,p\,(\nabla\cdot\boldsymbol{\xi})\,(\nabla\cdot\boldsymbol{\eta}) + \mu_0^{-1}\,\mathbf{Q}\cdot\mathbf{R} + \frac{1}{2}\,\nabla p\cdot[(\nabla\cdot\boldsymbol{\eta})\,\boldsymbol{\xi} + (\nabla\cdot\boldsymbol{\xi})\,\boldsymbol{\eta}] + \frac{1}{2}\,\mathbf{j}\cdot(\boldsymbol{\xi}\times\mathbf{R} + \boldsymbol{\eta}\times\mathbf{Q})\Big]dV_p + \int_{S_p}(\mathbf{n}\cdot\boldsymbol{\eta})\big(\Gamma\,p\,\nabla\cdot\boldsymbol{\xi} + \boldsymbol{\xi}\cdot\nabla p - \mu_0^{-1}\,\mathbf{B}\cdot\mathbf{Q}\big)dS_p, \tag{A1}$$

where $\mathbf{R} = \nabla\times(\boldsymbol{\eta}\times\mathbf{B})$, and use has been made of Eqs. (1) and (2). The surface integral can be expressed as

$$\int_{S_p}(\mathbf{n}\cdot\boldsymbol{\eta})\big(\Gamma\,p\,\nabla\cdot\boldsymbol{\xi} + \boldsymbol{\xi}\cdot\nabla p - \mu_0^{-1}\,\mathbf{B}\cdot\mathbf{Q}\big)dS_p = -\int_{S_p}(\mathbf{n}\cdot\boldsymbol{\eta})\,(\mathbf{n}\cdot\boldsymbol{\xi})\,\mathbf{n}\cdot\left[\!\!\left[\nabla\left(p + \frac{B^2}{2\,\mu_0}\right)\right]\!\!\right]dS_p + \mu_0^{-1}\int_{S_p}\mathbf{n}\cdot\mathbf{C}\times(\nabla\times\mathbf{A})\,dS_p, \tag{A2}$$

where use has been made of Eqs. (4), (8), and (9). However, the boundary conditions (10) and (11) allow us to write

$$\int_{S_p}\mathbf{n}\cdot\mathbf{C}\times(\nabla\times\mathbf{A})\,dS_p = -\int_V\nabla\cdot[\mathbf{C}\times(\nabla\times\mathbf{A})]\,dV = -\int_V(\nabla\times\mathbf{C})\cdot(\nabla\times\mathbf{A})\,dV, \tag{A3}$$

where use has been made of Eq. (7). Here, V denotes the appropriate vacuum region: i.e., V_i for the case of a perfectly conducting wall, and $V_{io} = V_i + V_o$ for the case of no wall. The previous three equations yield

$$\int_{V_p}\boldsymbol{\eta}\cdot\mathbf{F}(\boldsymbol{\xi})\,dV_p = -\int_{V_p}\left[\Gamma\,p\,(\nabla\cdot\boldsymbol{\xi})\,(\nabla\cdot\boldsymbol{\eta}) + \mu_0^{-1}\,\mathbf{Q}\cdot\mathbf{R} + \frac{1}{2}\,\nabla p\cdot[(\nabla\cdot\boldsymbol{\eta})\,\boldsymbol{\xi} + (\nabla\cdot\boldsymbol{\xi})\,\boldsymbol{\eta}] + \frac{1}{2}\,\mathbf{j}\cdot(\boldsymbol{\xi}\times\mathbf{R} + \boldsymbol{\eta}\times\mathbf{Q})\right]dV_p - \int_{S_p}(\mathbf{n}\cdot\boldsymbol{\eta})\,(\mathbf{n}\cdot\boldsymbol{\xi})\,\mathbf{n}\cdot\left[\!\!\left[\nabla\left(p + \frac{B^2}{2\,\mu_0}\right)\right]\!\!\right]dS_p - \int_V\mu_0^{-1}\,(\nabla\times\mathbf{C})\cdot(\nabla\times\mathbf{A})\,dV. \tag{A4}$$

The well-known self-adjoint property of the force operator,[8–11]

$$\int_{V_p}\boldsymbol{\eta}\cdot\mathbf{F}(\boldsymbol{\xi})\,dV_p = \int_{V_p}\boldsymbol{\xi}\cdot\mathbf{F}(\boldsymbol{\eta})\,dV_p, \tag{A5}$$

immediately follows from the invariance of Eq. (A4) under the transformation $\boldsymbol{\xi}$, $\mathbf{A}$, $\mathbf{Q}\leftrightarrow\boldsymbol{\eta}$, $\mathbf{C}$, $\mathbf{R}$, respectively.

2. Minimization of ΔW

Following from Sec. II E, we can write

$$\delta[\delta W(\boldsymbol{\xi},\boldsymbol{\xi})] = \delta W(\delta\boldsymbol{\xi},\boldsymbol{\xi}) + \delta W(\boldsymbol{\xi},\delta\boldsymbol{\xi}) = 2\,\delta W(\delta\boldsymbol{\xi},\boldsymbol{\xi}), \tag{A6}$$

where use has been made of the self-adjoint property of the force operator, (A5). It is easily demonstrated that

$$2\,\delta W_p(\delta\boldsymbol{\xi},\boldsymbol{\xi}) = -\int_{V_p} \delta\boldsymbol{\xi}\cdot\mathbf{F}(\boldsymbol{\xi})\,dV_p + \int_{S_p} (\mathbf{n}\cdot\delta\boldsymbol{\xi})\left(\Gamma\, p\,\nabla\cdot\boldsymbol{\xi} + \boldsymbol{\xi}\cdot\nabla p - \mu_0^{-1}\,\mathbf{B}\cdot\mathbf{Q}\right) dS_p, \tag{A7}$$

$$2\,\delta W_s(\delta\boldsymbol{\xi},\boldsymbol{\xi}) = \int_{S_p} (\mathbf{n}\cdot\delta\boldsymbol{\xi})\,\boldsymbol{\xi}\cdot\nabla\left(\frac{\hat{B}^2}{2\,\mu_0} - \frac{B^2}{2\,\mu_0} - p\right) dS_p, \tag{A8}$$

$$2\,\mu_0\,\delta W_v(\delta\mathbf{A},\mathbf{A}) = \int_{S_p} (\mathbf{n}\cdot\delta\boldsymbol{\xi})\,\hat{\mathbf{B}}\cdot(\nabla\times\mathbf{A})\,dS_p + \int_V \delta\mathbf{A}\cdot\nabla\times(\nabla\times\mathbf{A})\,dV. \tag{A9}$$

Here, use has been made of the boundary conditions (8), (10), and (11), which are assumed to apply to $\delta\boldsymbol{\xi}$ and $\delta\mathbf{A}$. Thus, setting $\delta[\delta W(\boldsymbol{\xi},\boldsymbol{\xi})] = 0$, we get

$$\begin{aligned} 0 = &-\int_{V_p} \delta\boldsymbol{\xi}\cdot\mathbf{F}(\boldsymbol{\xi})\,dV_p \\ &-\int_{S_p} (\mathbf{n}\cdot\delta\boldsymbol{\xi})\left[-\Gamma\, p\,\nabla\cdot\boldsymbol{\xi} + \boldsymbol{\xi}\cdot\nabla\left(\frac{B^2}{2\,\mu_0}\right) + \mu_0^{-1}\,\mathbf{B}\cdot\mathbf{Q}\right. \\ &\left. - \boldsymbol{\xi}\cdot\nabla\left(\frac{\hat{B}^2}{2\,\mu_0}\right) - \mu_0^{-1}\,\hat{\mathbf{B}}\cdot(\nabla\times\mathbf{A})\right] dS_p \\ &+\int_V \mu_0^{-1}\,\delta\mathbf{A}\cdot\nabla\times(\nabla\times\mathbf{A})\,dV. \end{aligned} \tag{A10}$$

Because the previous equation must hold for arbitrary $\delta\boldsymbol{\xi}$ and $\delta\mathbf{A}$, we deduce that the trial solution pair that minimizes δW satisfies the force-balance equation, $\mathbf{F}(\boldsymbol{\xi}) = \mathbf{0}$, in V_p, satisfies Eq. (7) in V, and also ought to satisfy the pressure balance matching condition, (9), at the plasma boundary.

3. Perfect-wall and no-wall stability

Suppose that the wall is perfectly conducting. In this case, the analysis of Sec. II E suggests that the minimum value of the perturbed potential energy can be written

$$\delta W_{pw} = \delta W_p + \delta W_s + \delta W_v^{(b)}, \tag{A11}$$

where δW_p and δW_s are calculated from a particular solution of Eq. (17) that is well-behaved at the magnetic axis, and

$$\delta W_v^{(b)} = \frac{1}{2\,\mu_0}\int_{V_i} (\nabla\times\mathbf{A}_{pw})^2\,dV_i. \tag{A12}$$

Here, the superscript (b) implies that the perfectly conducting wall is present at effective minor radius $\overline{b}$. Moreover, $\mathbf{A}_{pw}(\mathbf{r})$ is a solution of Eq. (7) that satisfies the boundary conditions

$$\mathbf{n}\times\mathbf{A}_{pw} = -(\mathbf{n}\cdot\boldsymbol{\xi})\,\hat{\mathbf{B}}, \tag{A13}$$

on S_p [see Eq. (8)], and

$$\mathbf{n}_w\times\mathbf{A}_{pw} = \mathbf{0}, \tag{A14}$$

on S_w. [See Eq. (10).]

Suppose that there is no wall. In this case, the analysis of Sec. II E suggests that the minimum value of the perturbed potential energy can be written as

$$\delta W_{nw} = \delta W_p + \delta W_s + \delta W_v^{(\infty)}, \tag{A15}$$

where δW_p and δW_s are calculated from the same solution of Eq. (17) as that used to calculate δW_{pw}, and

$$\delta W_v^{(\infty)} = \frac{1}{2\,\mu_0}\int_{V_{io}} (\nabla\times\mathbf{A}_{nw})^2\,dV_{io}. \tag{A16}$$

Here, the superscript (∞) implies that the perfectly conducting wall is absent, which is equivalent to it being placed at infinity. Moreover, $\mathbf{A}_{nw}(\mathbf{r})$ is a solution of Eq. (7) that satisfies the boundary conditions

$$\mathbf{n}\times\mathbf{A}_{nw} = -(\mathbf{n}\cdot\boldsymbol{\xi})\,\hat{\mathbf{B}}, \tag{A17}$$

on S_p [see Eq. (8)], and

$$\nabla\times\mathbf{A}_{nw} = \mathbf{0}, \tag{A18}$$

at infinity. [See Eq. (11).]

4. Self-adjoint property of force operator in presence of thick resistive wall

The proof of the self-adjoint property of the force operator in the presence of a thick resistive wall follows along the lines of that in Subsection 1 of Appendix, except that

$$\begin{aligned} &\int_{S_p} \mathbf{n}\cdot\mathbf{C}\times(\nabla\times\mathbf{A})\,dS_p \\ &= -\int_{V_i} \nabla\cdot[\mathbf{C}_i\times(\nabla\times\mathbf{A}_i)]\,dV_i + \int_{S_w} \mathbf{n}_w\cdot\mathbf{C}_i\times(\nabla\times\mathbf{A}_i)\,dS_w \\ &= -\int_{V_i} (\nabla\times\mathbf{C}_i)\cdot(\nabla\times\mathbf{A}_i)\,dV_i \\ &\quad -\int \mathbf{n}_w\times\mathbf{C}_i\cdot\mathbf{n}_w\times[\mathbf{n}_w\times(\nabla\times\mathbf{A}_i)]\,dS_w, \end{aligned} \tag{A19}$$

where use has been made of Eq. (7). However, Eq. (40) can easily be generalized to give

$$\begin{aligned} &\mathbf{n}_w\times\mathbf{C}_i\cdot\mathbf{n}_w\times[\mathbf{n}_w\times(\nabla\times\mathbf{A}_i)] \\ &= \mathbf{n}_w\times\mathbf{C}_o\cdot\mathbf{n}_w\times[\mathbf{n}_w\times(\nabla\times\mathbf{A}_o)] \\ &\quad + \frac{\lambda\tanh\lambda}{d}\,\mathbf{n}_w\times\mathbf{C}_i\cdot\mathbf{n}_w\times\mathbf{A}_i. \end{aligned} \tag{A20}$$

Moreover,

$$\int_{S_w} \mathbf{n}_w \times \mathbf{C}_o \cdot \mathbf{n}_w \times [\mathbf{n}_w \times (\nabla \times \mathbf{A}_o)]\, dS_w = -\int_{S_w} \mathbf{n}_w \times \mathbf{C}_o \cdot (\nabla \times \mathbf{A}_o)\, dS_w = \int_{V_o} \nabla \cdot [\mathbf{C}_o \times (\nabla \times \mathbf{A}_o)]\, dV_o = \int_{V_o} (\nabla \times \mathbf{C}_o) \cdot (\nabla \times \mathbf{A}_o)\, dV_o, \tag{A21}$$

where use has been made of Eqs. (7) and (11). Hence, we deduce that

$$\int_{S_p} \mathbf{n} \cdot \mathbf{C} \times (\nabla \times \mathbf{A})\, dS_p = -\int_{V_i} (\nabla \times \mathbf{C}_i) \cdot (\nabla \times \mathbf{A}_i)\, dV_i - \int_{V_o} (\nabla \times \mathbf{C}_o) \cdot (\nabla \times \mathbf{A}_o)\, dV_o - \int_{S_w} \frac{\lambda \tanh \lambda}{d}\, \mathbf{n}_w \times \mathbf{C}_i \cdot \mathbf{n}_w \times \mathbf{A}_i\, dS_w. \tag{A22}$$

Thus, in the presence of a thick resistive wall, Eq. (A4) generalizes to give

$$\begin{aligned}\int_{V_p} \boldsymbol{\eta} \cdot \mathbf{F}(\boldsymbol{\xi})\, dV_p = &-\int_{V_p} \left[\Gamma p\, (\nabla \cdot \boldsymbol{\xi})\, (\nabla \cdot \boldsymbol{\eta}) + \mu_0^{-1}\, \mathbf{Q} \cdot \mathbf{R} + \frac{1}{2}\, \nabla p \cdot [(\nabla \cdot \boldsymbol{\eta})\, \boldsymbol{\xi} + (\nabla \cdot \boldsymbol{\xi})\, \boldsymbol{\eta}] + \frac{1}{2}\, \mathbf{j} \cdot (\boldsymbol{\xi} \times \mathbf{R} + \boldsymbol{\eta} \times \mathbf{Q})\right] dV_p \\ &- \int_{S_p} (\mathbf{n} \cdot \boldsymbol{\eta})\, (\mathbf{n} \cdot \boldsymbol{\xi})\, \mathbf{n} \cdot \left[\left[\nabla\left(p + \frac{B^2}{2\,\mu_0}\right)\right]\right] dS_p - \int_{V_i} \mu_0^{-1} (\nabla \times \mathbf{C}_i) \cdot (\nabla \times \mathbf{A}_i)\, dV_i - \int_{V_o} \mu_0^{-1}\, (\nabla \times \mathbf{C}_o) \cdot (\nabla \times \mathbf{A}_o)\, dV_o \\ &- \int_{S_w} \mu_0^{-1}\, \frac{\lambda \tanh \lambda}{d}\, \mathbf{n}_w \times \mathbf{C}_i \cdot \mathbf{n}_w \times \mathbf{A}_i\, dS_w.\end{aligned} \tag{A23}$$

The self-adjoint property of the force operator, (A5), immediately follows from the symmetric nature of the previous equation. Thus, we conclude that the force operator remains self-adjoint in the presence of a resistive wall, even when the wall lies in the thick-shell limit.

5. Minimization of δW in presence of thick resistive wall

Consider the expression for $\delta W(\boldsymbol{\xi}, \boldsymbol{\xi})$ given in Eq. (41). We can write

$$\delta[\delta W(\boldsymbol{\xi}, \boldsymbol{\xi})] = \delta W(\delta\boldsymbol{\xi}, \boldsymbol{\xi}) + \delta W(\boldsymbol{\xi}, \delta\boldsymbol{\xi}) = 2\, \delta W(\delta\boldsymbol{\xi}, \boldsymbol{\xi}), \tag{A24}$$

where use has been made of the self-adjoint property of the force operator, (A5). Now, $2\,\delta W_p(\boldsymbol{\xi}, \boldsymbol{\xi})$ and $2\,\delta W_s(\delta\boldsymbol{\xi}, \boldsymbol{\xi})$ are given by Eqs. (A7) and (A8), respectively. Moreover,

$$\begin{aligned}2\,\mu_0\, \delta W_v^{(i)}(\delta\mathbf{A}_i, \mathbf{A}_i) &= \int_{V_i} \nabla \times \delta\mathbf{A}_i \cdot \nabla \times \mathbf{A}_i\, dV_i = \int_{V_i} \left\{\nabla \cdot [\delta\mathbf{A}_i \times (\nabla \times \mathbf{A}_i)] + \delta\mathbf{A}_i \cdot \nabla \times (\nabla \times \mathbf{A}_i)\right\} dV_i \\ &= -\int_{S_p} \mathbf{n} \cdot \delta\mathbf{A} \times (\nabla \times \mathbf{A})\, dS_p + \int_{S_w} \mathbf{n}_w \cdot \delta\mathbf{A}_i \times (\nabla \times \mathbf{A}_i)\, dS_w + \int_{V_i} \delta\mathbf{A}_i \cdot \nabla \times (\nabla \times \mathbf{A}_i)\, dV_i \\ &= \int_{S_p} (\mathbf{n} \cdot \boldsymbol{\xi})\, \hat{\mathbf{B}} \cdot (\nabla \times \mathbf{A})\, dS_p - \int_{S_w} \mathbf{n}_w \times \boldsymbol{\delta}\mathbf{A}_i \cdot \mathbf{n}_w \times [\mathbf{n}_w \times (\nabla \times \mathbf{A}_i)]\, dS_w + \int_{V_i} \delta\mathbf{A}_i \cdot \nabla \times (\nabla \times \mathbf{A}_i)\, dV_i,\end{aligned} \tag{A25}$$

where use has been made of the essential boundary condition (8). Furthermore,

$$\begin{aligned}2\,\mu_0\, \delta W_v^{(o)}(\delta\mathbf{A}_o, \mathbf{A}_o) &= \int_{V_o} \nabla \times \delta\mathbf{A}_o \cdot \nabla \times \mathbf{A}_o\, dV_o = \int_{V_o} \left\{\nabla \cdot [\delta\mathbf{A}_o \times (\nabla \times \mathbf{A}_o)] + \delta\mathbf{A}_o \cdot \nabla \times (\nabla \times \mathbf{A}_o)\right\} dV_o \\ &= -\int_{S_w} \mathbf{n}_w \cdot \delta\mathbf{A}_o \times (\nabla \times \mathbf{A}_o)\, dS_w + \int_{V_o} \delta\mathbf{A}_o \cdot \nabla \times (\nabla \times \mathbf{A}_o)\, dV_o = \int_{S_w} \mathbf{n}_w \times \boldsymbol{\delta}\mathbf{A}_i \cdot \frac{\mathbf{n}_w \times [\mathbf{n}_w \times (\nabla \times \mathbf{A}_o)]}{\cosh \lambda}\, dS_w \\ &\quad + \int_{V_o} \delta\mathbf{A}_i \cdot \nabla \times (\nabla \times \mathbf{A}_o)\, dV_o,\end{aligned} \tag{A26}$$

where use has been made of the essential boundary condition (11), as well as Eq. (37). Finally,

$$2\,\mu_0\, \delta W_v^{(w)}(\delta\mathbf{A}_i, \mathbf{A}_i) = \int_{S_w} \frac{\lambda \tanh \lambda}{d}\, \mathbf{n}_w \times \delta\mathbf{A}_i \cdot \mathbf{n}_w \times \mathbf{A}_i\, dS_w. \tag{A27}$$

Thus, setting $\delta[\delta W(\boldsymbol{\xi}, \boldsymbol{\xi})]$ to zero, we obtain

$$\begin{aligned}0 = &-\int_{V_p} \delta\boldsymbol{\xi} \cdot \mathbf{F}(\boldsymbol{\xi})\, dV_p - \int_{S_p} (\mathbf{n} \cdot \delta\boldsymbol{\xi}) \left[-\Gamma p\, \nabla \cdot \boldsymbol{\xi} + \boldsymbol{\xi} \cdot \nabla\left(\frac{B^2}{2\,\mu_0}\right) + \mu_0^{-1}\, \mathbf{B} \cdot \mathbf{Q} - \boldsymbol{\xi} \cdot \nabla\left(\frac{\hat{B}^2}{2\,\mu_0}\right) - \mu_0^{-1}\, \hat{\mathbf{B}} \cdot (\nabla \times \mathbf{A})\right] dS_p + \int_{V_i} \mu_0^{-1}\, \delta\mathbf{A}_i \cdot \nabla \\ &\times (\nabla \times \mathbf{A}_i)\, dV_i + \int_{V_o} \mu_0^{-1} \delta\mathbf{A}_o \cdot \nabla \times (\nabla \times \mathbf{A}_o)\, dV_o + \mu_0^{-1} \int_{S_w} \mathbf{n}_w \times \delta\mathbf{A}_i \\ &\cdot \left[\frac{\mathbf{n}_w \times [\mathbf{n}_w \times (\nabla \times \mathbf{A}_o)]}{\cosh \lambda} - \mathbf{n}_w \times [\mathbf{n}_w \times (\nabla \times \mathbf{A}_i)] + \frac{\lambda \tanh \lambda}{d}\, \mathbf{n}_w \times \mathbf{A}_i\right].\end{aligned} \tag{A28}$$

However, the previous equation must hold for arbitrary $\delta\boldsymbol{\xi}$ and $\delta\mathbf{A}$. Hence, we deduce that the solution pair $[\boldsymbol{\xi}(\mathbf{r}), \mathbf{A}(\mathbf{r})]$, that minimizes the $\delta W(\boldsymbol{\xi}, \boldsymbol{\xi})$ specified in Eq. (41) satisfies Eq. (17) in V_p, satisfies Eq. (7) in V_i and V_o, satisfies the pressure balance matching condition, (9), at the plasma boundary, and satisfies the matching condition (39) at the wall.

6. Useful results

Making use of the analysis of Sec. III C, the following results are easily demonstrated:

$$2\,\mu_0\,\delta W_v^{(i)} = \int_{S_p} (\mathbf{n}\cdot\boldsymbol{\xi})\,\hat{\mathbf{B}}\cdot\nabla\times\mathbf{A}_i\,dS_p + \int_{S_w}\mathbf{n}_w\times\mathbf{A}_i\cdot\nabla\times\mathbf{A}_i\,dS_w = c_1\int_{S_p}(\mathbf{n}\cdot\boldsymbol{\xi})\,\hat{\mathbf{B}}\cdot\nabla\times\mathbf{A}_{nw}\,dS_p + c_2\int_{S_p}(\mathbf{n}\cdot\boldsymbol{\xi})\,\hat{\mathbf{B}}\cdot\nabla\times\mathbf{A}_{pw}\,dS_p$$
$$+ c_1^2\int_{S_w}\mathbf{n}_w\times\mathbf{A}_{nw}\cdot\nabla\times\mathbf{A}_{nw}\,dS_w + c_1\,c_2\int_{S_w}\mathbf{n}_w\times\mathbf{A}_{nw}\cdot\nabla\times\mathbf{A}_{pw}\,dS_w, \tag{A29}$$

$$2\,\mu_0\,\delta W_v^{(o)} = -\int_{S_w}\mathbf{n}_w\times\mathbf{A}_o\cdot\nabla\times\mathbf{A}_o\,dS_w = -c_3^2\int_{S_w}\mathbf{n}_w\times\mathbf{A}_{nw}\cdot\nabla\times\mathbf{A}_{nw}\,dS_w, \tag{A30}$$

$$2\,\mu_0\,\delta W_v^{(b)} = \int_{S_p}(\mathbf{n}\cdot\boldsymbol{\xi})\,\hat{\mathbf{B}}\cdot\nabla\times\mathbf{A}_{pw}\,dS_p, \tag{A31}$$

$$2\,\mu_0\,\delta W_v^{(\infty)} = \int_{S_p}(\mathbf{n}\cdot\boldsymbol{\xi})\,\hat{\mathbf{B}}\cdot\nabla\times\mathbf{A}_{nw}\,dS_p, \tag{A32}$$

and

$$\int_{V_i}(\nabla\times\mathbf{A}_{nw})\cdot(\nabla\times\mathbf{A}_{pw})\,dV_i = \int_{S_p}(\mathbf{n}\cdot\boldsymbol{\xi})\,\hat{\mathbf{B}}\cdot\nabla\times\mathbf{A}_{pw}\,dS_p + \int_{S_w}\mathbf{n}_w\times\mathbf{A}_{nw}\cdot\nabla\times\mathbf{A}_{pw}\,dS_w = \int_{S_p}(\mathbf{n}\cdot\boldsymbol{\xi})\,\hat{\mathbf{B}}\cdot\nabla\times\mathbf{A}_{nw}\,dS_p, \tag{A33}$$

where use has been made of Eqs. (7), (8), (10), (11), (A13), (A14), (A17), (A18), (47), and (48). It is helpful to define

$$2\,\mu_0\,\delta W_v^{(x)} = \int_{V_o}|\nabla\times\mathbf{A}_{nw}|^2\,dV_p = -\int_{S_w}\mathbf{n}\times\mathbf{A}_{nw}\cdot\nabla\times\mathbf{A}_{nw}\,dS_w. \tag{A34}$$

Here, $\delta W_v^{(x)}$ represents the contribution of the region V_o to the no-wall vacuum energy.

7. Minimization of δW_p in axisymmetric plasma

In an axisymmetric quasi-cylindrical plasma, the perturbed plasma potential energy can be written[9–11]

$$\delta W_p = \frac{1}{2\,\mu_0}\int_0^a\left[\Gamma\,\mu_0\,p\,(\nabla\cdot\boldsymbol{\xi}^*)\,(\nabla\cdot\boldsymbol{\xi}) + \mathbf{Q}^*\cdot\mathbf{Q} + (\nabla\cdot\boldsymbol{\xi}_\perp^*)\,[\boldsymbol{\xi}_\perp\cdot\nabla(\mu_0\,p)] + \mu_0\,\mathbf{j}\cdot\boldsymbol{\xi}_\perp^*\times\mathbf{Q}\right]\frac{1}{2}\,2\pi\,r\,2\pi\,R_0\,dr, \tag{A35}$$

where $\mu_0\,\mathbf{j} = \nabla\times\mathbf{B}$, $\mathbf{Q} = \nabla\times(\boldsymbol{\xi}_\perp\times\mathbf{B})$, and the factor 1/2 comes from averaging $\cos^2(m\,\theta + k\,z)$. After a great deal of standard analysis, we arrive at

$$\delta W_p = \frac{\pi^2\,R_0}{\mu_0}\int_0^a W(r)\,r\,dr, \tag{A36}$$

where

$$W(r) = \Gamma\,\mu_0\,p\left|\frac{(r\,\xi)\prime}{r} + \mathrm{i}\,\frac{G}{B}\,\eta + \mathrm{i}\,\frac{F}{B}\,\xi_\parallel\right|^2 + \left|\frac{G}{k_0}\,\frac{(r\,\xi)\prime}{r} + \frac{2\,k\,B_\theta}{r\,k_0}\,\xi + \mathrm{i}\,k_0\,B\,\eta\right|^2 + A_1\,\xi'^2 + A_2\,\xi'\,\xi + A_3\,\xi^2, \tag{A37}$$

and

$$A_1(r) = \frac{F^2}{k_0^2}, \tag{A38}$$

$$A_2(r) = \frac{(k^2\,r^2\,B_z^2 - m^2\,B_\theta^2)}{r^3\,k_0^2}, \tag{A39}$$

$$A_3(r) = F^2 + \frac{1}{r^2}\left[B_z^2 - B_\theta^2 - 2\,r\,B_\theta'\,B_\theta - \frac{(r\,G^2 + 4\,m\,k\,B_\theta\,B_z)}{r\,k_0^2}\right], \tag{A40}$$

$$G(r) = \frac{m}{r}\,B_z - k\,B_\theta, \tag{A41}$$

$$F(r) = \frac{m}{r}\,B_\theta + k\,B_z, \tag{A42}$$

$$k_0^2(r) = \frac{m^2}{r^2} + k^2. \tag{A43}$$

Because $\xi_\parallel$ and η only appear in Eq. (A37) inside positive-definite terms, we can minimize δW_p by choosing $\xi_\parallel$ and η in such a manner as to set these terms to zero. After doing this, and after integrating by parts, we arrive at Eqs. (77)–(79).

8. Minimization of δW in axisymmetric plasma

The total potential energy of the perturbation is

$$\begin{aligned}\delta W &= \delta W_p + \delta W_s + \delta W_v^{(i)} + \delta W_w + \delta W_v^{(o)}\\ &= \frac{\pi^2 R_0}{\mu_0}\left\{\int_0^a (f\,\xi'^2 + g\,\xi^2)\,dr + \left[\left(\frac{k^2 r^2 B_z^2 - m^2 B_\theta^2}{k_0^2 r^2}\right)\xi^2\right.\right.\\ &\quad \left. + (B_\theta^2 - \hat{B}_\theta^2)\,\xi^2 - r\hat{F}\,\xi\,V\right]_a - \int_a^{b_-} V\nabla^2 V\,r\,dr + \left(r\frac{dV}{dr}\right)_{b_-}\\ &\quad \times\left[V(b_-) + \frac{\lambda\tanh\lambda}{d}\frac{1}{k_b^2}\left(\frac{dV}{dr}\right)_{b_-} - \frac{V(b_+)}{\cosh\lambda}\right] - \left.\int_{b_+}^{\infty} V\nabla^2 V\,r\,dr\right\}.\end{aligned} \tag{A44}$$

Here, use has been made of the essential boundary condition (87). If we minimize the potential energy, making use of the self-adjoint property of the overall expression demonstrated in Subsection 4 of Appendix, then we get

$$\begin{aligned}\delta[\delta W] &= \frac{2\pi^2 R_0}{\mu_0}\left\{\int_0^a \delta\xi\left[-(f\,\xi')' + g\,\xi\right]dr\right.\\ &\quad + \delta\xi(a)\left[f\,\xi' + \left(\frac{k^2 r^2 B_z^2 - m^2 B_\theta^2}{k_0^2 r^2}\right)\xi + (B_\theta^2 - \hat{B}_\theta^2)\,\xi - r\hat{F}\,V\right]_a\\ &\quad - \int_a^{b_-}\delta V\nabla^2 V\,r\,dr + \left(r\frac{d\delta V}{dr}\right)_{b_-}\\ &\quad \times\left[V(b_-) + \frac{\lambda\tanh\lambda}{d}\frac{1}{k_b^2}\left(\frac{dV}{dr}\right)_{b_-} - \frac{V(b_+)}{\cosh\lambda}\right]\\ &\quad \left. - \int_{b_+}^{\infty}\delta V\nabla^2 V\,r\,dr\right\} = 0.\end{aligned} \tag{A45}$$

Given that the previous expression must hold for arbitrary $\delta\xi$ and δV, we deduce that the perturbation that minimizes δW satisfies Eq. (92) in the plasma, satisfies (93) in the vacuum, and satisfies the natural boundary conditions (86) and (88) at the plasma boundary and at the wall, respectively.

REFERENCES

[1] G. Laval, R. Pellat, and J. S. Soule, Phys. Fluids **17**, 835 (1974).
[2] R. L. Dewar, R. C. Grimm, J. L. Johnson, E. A. Frieman, J. M. Greene, and P. H. Rutherford, Phys. Fluids **17**, 930 (1974).
[3] F. A. Haas, Nucl. Fusion **15**, 407 (1975).
[4] J. A. Wesson, *Tokamaks*, 4th ed. (Oxford University Press, Oxford, UK, 2011).
[5] R. Fitzpatrick, *Tearing Mode Dynamics in Tokamak Plasmas* (IOP, Bristol, UK, 2023).
[6] D. Pfirsch and H. Tasso, Nucl. Fusion **11**, 259 (1971).
[7] J. P. Goedbloed, D. Pfirsch, and H. Tasso, Nucl. Fusion **12**, 649 (1972).
[8] I. B. Bernstein, E. A. Frieman, M. D. Kruskal, and R. M. Kulsrud, Proc. R. Soc. London, Ser. A **244**, 17 (1958).
[9] J. P. Freidberg, Rev. Mod. Phys. **54**, 801 (1982).
[10] J. P. Freidberg, *Ideal Magnetohydrodynamics* (Plenum, New York, 1987).
[11] J. P. Goedbloed and S. Poedts, *Principles of Magnetohydrodynamics* (Cambridge University Press, Cambridge, UK, 2004).
[12] S. W. Haney and J. P. Freidberg, Phys. Fluids B **1**, 1637 (1989).
[13] C. G. Gimblett, Nucl. Fusion **26**, 617 (1986).
[14] R. Fitzpatrick, S. C. Guo, D. J. Den Hartog, and C. C. Hegna, Phys. Plasmas **6**, 3878 (1999).
[15] B. E. Chapman, R. Fitzpatrick, D. Craig, P. Martin, and G. Spizzo, Phys. Plasmas **11**, 2156 (2004).
[16] L.-J. Zheng and M. T. Kotschenreuther, Phys. Plasmas **12**, 072504 (2005).
[17] V. D. Pustovitov, Phys. Plasmas **19**, 062503 (2012).
[18] R. Fitzpatrick, Phys. Plasmas **20**, 012504 (2013).
[19] N. D. Lepikhin and V. D. Pustovitov, Phys. Plasmas **21**, 042504 (2014).
[20] J. D. Jackson, *Classical Electrodynamics*, 3rd ed. (Wiley & Sons, Hoboken, NJ, 1998).
[21] W. A. Newcomb, Ann. Phys. **10**, 232 (1960).
[22] R. Fitzpatrick, Phys. Plasmas **6**, 1168 (1999).
[23] J. W. Berkery, R. Betti, Y. Q. Liu, and S. A. Sabbagh, Phys. Plasmas **30**, 120901 (2023).
[24] R. Betti and J. P. Freidberg, Phys. Rev. Lett. **74**, 2949 (1995).
[25] L. J. Zheng, M. Kotschenreuther, and M. S. Chu, Phys. Rev. Lett. **95**, 255003 (2005).
[26] B. Hu and R. Betti, Phys. Rev. Lett. **93**, 105002 (2004).
[27] B. Hu, R. Betti, and J. Manickam, Phys. Plasmas **12**, 057301 (2005).
[28] A. Bondeson and D. Ward, Phys. Rev. Lett. **72**, 2709 (1994).
[29] J.-K. Park, Phys. Plasmas **18**, 110702 (2011).
[30] R. Fitzpatrick, Phys. Plasmas **31**, 102507 (2024).
[31] R. Fitzpatrick, R. J. Hastie, T. J. Martin, and C. M. Roach, Nucl. Fusion **33**, 1533 (1993).